Since January 2020 Elsevier has created a COVID-19 resource centre with free information in English and Mandarin on the novel coronavirus COVID-19. The COVID-19 resource centre is hosted on Elsevier Connect, the company's public news and information website.

Elsevier hereby grants permission to make all its COVID-19-related research that is available on the COVID-19 resource centre - including this research content - immediately available in PubMed Central and other publicly funded repositories, such as the WHO COVID database with rights for unrestricted research re-use and analyses in any form or by any means with acknowledgement of the original source. These permissions are granted for free by Elsevier for as long as the COVID-19 resource centre remains active.

ADVANCES IN VIRUS RESEARCH, VOL 63

GENOMIC ORGANIZATION, BIOLOGY, AND DIAGNOSIS OF TAURA SYNDROME VIRUS AND YELLOWHEAD VIRUS OF PENAEID SHRIMP

Arun K. Dhar,[*] Jeff A. Cowley,[†] Kenneth W. Hasson,[‡] and Peter J. Walker[†]

[*]Department of Biology, San Diego State University
San Diego, California 92182
[†]CSIRO Livestock Industries, Queensland Bioscience Precinct
St. Lucia, Queensland 4067
[‡]Texas Veterinary Medical Diagnostic Laboratory
College Station, Texas 77841

I. Introduction

Over the past two decades, shrimp aquaculture has transformed into a major industry worldwide, providing jobs for millions of people directly and indirectly. As shrimp farming expands globally, it faces a growing number of challenges. Among these, diseases caused by viruses have been recognized as a major threat to the long-term sustainability of this industry. The first shrimp virus was isolated by Couch from wild shrimp (*Penaeus duorarum*) collected from the Florida Gulf Coast in the early 1970s (Couch, 1974a,b). Since then, more than 20

Copyright 2004, Elsevier Inc.
All rights reserved.
0065-3527/04 $35.00

viruses have been reported to infect shrimp (Lightner, 1996a), and the list is growing. Many of these viruses have caused serious diseases in penaeid shrimp, resulting in significant economic losses to commercial shrimp farmers. The three most detrimental shrimp viruses are white spot syndrome virus (WSSV), yellowhead virus (YHV), and Taura syndrome virus (TSV), all of which have caused serious epizootics in various regions of Asia and are considered notifiable by the Office International de Epizooties (OIE, 2002). In the Western Hemisphere, the shrimp industry has suffered catastrophic losses due to both WSSV and TSV; however, losses due to YHV have not been reported (Lightner *et al.*, 1997b; Tu *et al.*, 1999; Yu and Song, 2000). Several reviews describing the histopathology, diagnostic methods, and epidemiology of these important viral disease have been published in recent years (Flegel, 1997; Lightner, 1996b; Lightner and Redman, 1998; Loh *et al.*, 1997). These are valuable references for researchers interested in shrimp viruses. The present review is focused on two viruses, TSV and YHV, with a major emphasis on the genome organization of these viruses.

II. Taura Syndrome Disease

A. History

The designation of TSV, the causative agent of Taura syndrome (TS), as a notifiable disease by the OIE amply reflects the serious nature of this viral agent and the deleterious economic impact it has inflicted on shrimp farming in the Americas (Brock, 1997; Brock *et al.*, 1995, 1997; Hasson *et al.*, 1995, 1999a,b; Lightner, 1995, 1996a,b; Lightner *et al.*, 1995, 1997a,b; OIE, 2002) and, more recently, in Taiwan (Tu *et al.*, 1999; Yu and Song, 2000). Of the approximately 20 known viral diseases of penaeid shrimp, TS is possibly one of the most controversial in terms of its disputed etiology (Brock *et al.*, 1995; Hasson, 1998; Hasson *et al.*, 1995, 1999a,b; Lightner, 1996a,b, 1998, 1999). Hence, a review of this disease would be incomplete without explaining the cause of this dispute and how it contributed to the unobstructed spread of TSV throughout the Western Hemisphere between 1992 to 1996 (Hasson *et al.*, 1999a). The resulting panzootic cost to the shrimp farming industry in the Americas was an estimated $1.2–2 billion in lost revenue (Brock, 1997; Hasson, 1998; Hasson *et al.*, 1999a; Lightner, 1995, 1996; Lightner *et al.*, 1995, 1996b).

Ecuadorian investigators first recognized TS as a new disease, both clinically and histologically, in Pacific white shrimp (*Penaeus*

vannamei) farms located along the mouth of the Taura river basin (Guayas Province, Ecuador) during the summer of 1992 (Brock *et al*., 1995, 1997; Jimenez, 1992; Lightner *et al*., 1994; Wigglesworth, 1994). They named the disease after the Taura region where the first outbreaks were detected (Jimenez, 1992; Wigglesworth, 1994). The cause of TS was initially attributed to the toxic effects of two systemic fungicides: Tilt (Propicanizole, Ciba-Geigy) and Calixin (Tridemorph, BASF). These fungicides were being sprayed on local banana plantations to control Black Leaf Wilt disease, a serious banana plant fungal infection (Brock *et al*., 1995; Hasson, 1998; Intriago *et al*., 1997a,b; Lightner *et al*., 1994; Stern, 1995; Wigglesworth, 1994). Because initial disease occurrence in adjacent shrimp farms coincided with periods of heavy rainfall, it was assumed that fungicide-contaminated runoff from the plantations was the direct cause of the shrimp die-offs (Jimenez, 1992; Lightner *et al*., 1994; Wigglesworth, 1994). This hypothesized toxic etiology for the shrimp losses persisted in the popular press through early 1995. No confirmatory scientific evidence, however, was forthcoming to support this theory (Anonymous, 1995; Barniol, 1995; Brock *et al*., 1995; Hasson, 1998; Hasson *et al*., 1995; Intriago *et al*., 1995a,b; Jimenez *et al*., 1995; Lightner *et al*., 1994, 1995). During the 2 years following its discovery, TS spread west through Ecuador's most concentrated shrimp farming region, southward into *P. vannamei* farms of Northern Peru, and northward into *P. vannamei* farms located on the Pacific Coast of Colombia (Brock *et al*., 1995; Hasson *et al*., 1999a; Lightner *et al*., 1994; Wigglesworth, 1994). In these latter two regions, there were neither banana plantations nor application of the two accused fungicides. All prior and subsequent attempts to experimentally induce TS by either water borne, oral, or injection-mediated exposure to Tilt and Calixin failed to reproduce the clinical signs and histological lesions associated with the disease (Brock *et al*., 1995, 1997; Hasson, 1998; Hasson *et al*., 1995; Lightner, 1996a; Lightner *et al*., 1994, 1995, 1996c). As a result, investigators began to question the toxic etiology hypothesis and pursue other possible causes. A third widely used banana plant fungicide in Ecuador, called Benlate O. D. (Benomyl, DuPont), was also tested as a possible cause of TS and, as with Tilt and Calixin, failed to induce the disease (Lightner *et al*., 1996c). During May 1994, two separate outbreaks of TS occurred among cultured *P. vannamei* on Oahu, Hawaii, representing the first incursion of this disease into the United States (Brock *et al*., 1995). Within 5 months of these two outbreaks, experimental *per os* induction of the disease was accomplished (Brock *et al*., 1995), a previously uncharacterized virus (named Taura syndrome virus) was

independently identified by two separate labs within the United States (Brock *et al.*, 1995; Hasson *et al.*, 1995; Lightner *et al.*, 1995), and the newly recognized virus was then shown to be the cause of TS through fulfillment of River's postulates (Hasson *et al.*, 1995). Although a viral etiology for TS had now been scientifically established, leaders of the Ecuadorian shrimp farming industry maintained that the disease had a toxic etiology in support of their ongoing litigation against the producers of Tilt (Ciba-Geigy, personal communication, 1995). The conflicting information regarding the etiology of TS left shrimp growers throughout the Americas confused or indifferent about the true causative nature of the disease, and no regulations to restrict international movement of live shrimp stocks were implemented. As a result, the disease was spread throughout the Western Hemisphere through sales of TSV-infected postlarvae and broodstock. At the end of 1996, 13 of the 14 shrimp farming countries in the Americas were infected with TSV (Brock *et al.*, 1995; Hasson, 1998; Hasson *et al.*, 1999a; Lightner, 1995, 1996a; Zarain-Herzberg and Ascencio-Valle, 2001). In 1999, Ecuadorian researchers conceded that TSV had been present in Ecuador since 1994 but maintained that the shrimp losses suffered by their industry during 1992 and 1993 were caused by toxic fungicides (Intriago *et al.*, 1997a,b; Jimenez *et al.*, 2000). This was contrary to the fact that these early outbreaks were clinically and histologically identical to TSV-induced epizootics and scientifically demonstrated to be TSV-caused (Bonami *et al.*, 1997; Brock *et al.*, 1995; Hasson *et al.*, 1995, 1999a; Lightner, 1995, 1996a, 1998; Lightner *et al.*, 1995). During 1999, the Ecuadorian shrimp farming community abandoned their position that Tilt and Calixin were the cause of TS and currently claim that the fungicide, Benlate O.D., is the actual etiologic agent of the disease. Thus, the ongoing controversy persists and now moves into its eleventh year.

B. Clinical Signs, Transmission, and Disease Cycle

1. Clinical Signs

The clinical signs of acute TSV infection in farmed *P. vannamei* include lethargy, anorexia, opaque musculature, atactic swimming behavior, flaccid bodies, soft cuticles, and chromatophore expansion resulting in reddening of the uropods, appendages, and general body (Brock *et al.*, 1995; Hasson *et al.*, 1995; Lightner, 1995, 1996a; Lightner *et al.*, 1994, 1995) (Fig. 1). Development of red coloration from chromatophore expansion is believed to be linked to pigment (carotenoids) incorporation resulting from the consumption of phytoplankton and is

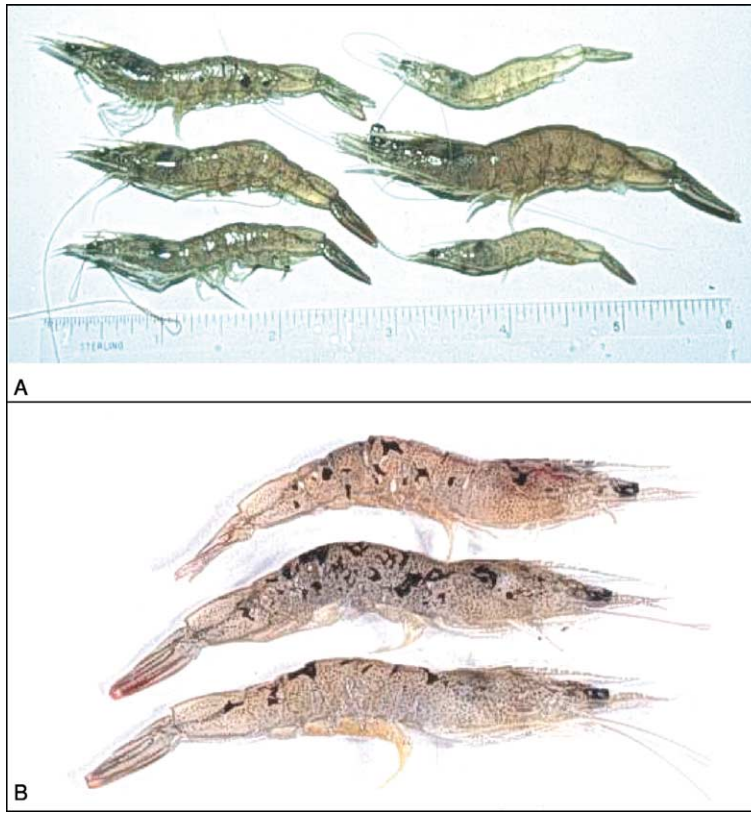

FIG 1. Farmed *Penaeus vannamei* juveniles originating from two separate TSV epizootics. (A) Signs of TSV acute phase infection. The shrimp in the upper right corner is healthy and translucent. The remaining five shrimp are acutely infected with TSV and display an overall darker coloration, typically ranging from lavender to red, due to chromatophore expansion (B) Signs of TSV transition phase infection. The cephalothorax and tail of these three shrimp display multifocal melanized lesions that indicate a transition phase TSV infection. These lesions identify foci of cuticular epithelium that were destroyed during the acute phase infection and are now in the process of resolving.

not observed in experimentally infected *P. vannamei* that are maintained in clear water systems on artificial diets (Brock *et al*., 1995; Hasson *et al*., 1995; Lightner *et al*., 1994, 1995). Naturally and experimentally infected shrimp that survive the acute phase infection develop grossly visible, multifocal, melanized lesions on the cephalothorax, tail, and appendages (Brock *et al*., 1995; Hasson *et al*., 1995; Lightner *et al*., 1994) (Fig. 1).

These lesions are characteristic of a transition phase of TSV infection (Hasson *et al.*, 1999b) (Section II,B,3). TSV typically strikes *P. vannamei* in late postlarval to early juvenile stages between 15 to 40 days poststocking of production or nursery ponds, but TSV is also capable of causing serious disease in subadult and adult *P. vannamei* (Brock *et al.*, 1995; Lightner, 1996a; Lightner *et al.*, 1994; Lotz, 1997; Wigglesworth, 1994). Infected *P. vannamei* generally die within 1 week of disease onset with cumulative mortalities typically ranging from 60 to 95% (Brock *et al.*, 1995, 1997; Hasson *et al.*, 1995; Lightner, 1995, 1996a; Lightner *et al.*, 1994, 1995; Wigglesworth, 1994). As with other mass mortalities in shrimp farms, whether due to an infectious or noninfectious agent, the flocking of sea birds over a stricken pond as they feed on the numerous dead and dying shrimp often signals a TSV epizootic (Brock *et al.*, 1997; Garza *et al.*, 1997). Similar TSV clinical signs and mortality data have been reported for *P. stylirostris* (Pacific blue shrimp) stocks (Robles-Sikisaka *et al.*, 2002) that were widely farmed in Mexico during 1996 to 2000 (Clifford, 2000) and, prior to 1999, considered TSV resistant (Brock *et al.*, 1995). Robles-Sikisaka *et al.* (2002) and Erickson *et al.* (2002) demonstrated that TSV epizootics among *L. stylirostris* stocks in Mexico were the result of a new emerging strain or serotype of TSV (Section II,F).

2. *Transmission*

The different modes of TSV transmission have been examined to a limited extent (Table I). Vertical transmission of this virus has been hypothesized to occur based on anecdotal information but not

TABLE I
VECTORS OF TSV

A. Short-range transmission (within ponds)
• Cannibalism of acute or chronically infected moribund or dead shrimp
• Waterborne
B. Medium-range transmission (between ponds and farms)
• Sea birds
• Water boatmen (*T. reticulata*)
• Chronically infected shrimp
• Wild infected postlarvae
C. Long-range transmission (between countries)
• Live infected postlarvae and broodstock
• Frozen infected shrimp

demonstrated (Lightner, 1995; Lightner and Redman, 1998). Dissemination of the virus within a pond or tank results from cannibalism of infected moribund or dead shrimp by healthy shrimp, resulting in rapid exponential spread of the virus within the exposed population (Brock *et al*., 1995; Hasson *et al*., 1995). Work by Prior and Browdy (2000) showed that TSV remains pathogenic in decaying *P. vannamei* shrimp carcasses for up to 3 weeks following death and can serve as a source for renewed outbreaks if consumed by TSV-susceptible shrimp. In the same study, water borne transmission of TSV was demonstrated to occur for up to 48 hr following the peak mortality period of an experimentally induced TSV epizootic. Chronically infected *P. vannamei* harbor infectious TSV within both the lymphoid organ (LO) and hemolymph for at least 8–12 months postinfection, representing a potential source of renewed outbreaks if cannibalized (Hasson, 1998; Hasson *et al*., 1995, 1999c). As a result, persistence of TSV in a farm or a given region may be due to the presence of chronically infected shrimp living within ponds, canals, or adjacent estuaries.

The transmission of TSV between ponds or farms has been attributed to seabirds, predominantly gulls, and a flying aquatic insect commonly known as the water boatmen *(Trichocorixa reticulata)* (Garza *et al*., 1997; Hasson *et al*., 1995; Lightner, 1995, 1996a). Garza *et al*. (1997) demonstrated that sea gull feces collected from the banks of TSV infected ponds in Texas during the 1995 TSV epizootic contained infectious TSV. They hypothesized that shrimp eating birds transmit TSV to other ponds or farms through defecation of TSV infected feces with subsequent ingestion of the infected fecal matter by scavenging shrimp. Water boatmen are commonly found in large numbers in shrimp farms. They possess a sucking proboscis and will prey on small postlarval shrimp (Hasson *et al*., 1995; Lightner, 1995, 1996a,b). Limited histological and TSV *in situ* hybridization (ISH) analyses of experimentally exposed and wild water boatmen samples indicate that these insects transport TSV within their intestinal contents but are not directly infected by the virus (Hasson, unpublished data; Lightner, 1996a,b). Similar to sea birds, water boatmen are believed to be capable of disseminating infectious virus through their fecal matter, or, perhaps they spread the virus upon death when they are consumed by shrimp. Similar to the water boatmen, red drum (*Sciaenops ocellatus*), blue crabs (*Callinectes sapidus*), grass shrimp (*Palaemontes* sp.), and sea trout (*Cynoscion nebulosus*) are not infected by the virus as indicated by experimental TSV *per os* exposure and histologica analyses (Erickson *et al*., 1997). However, the possibility of fecal transmission of TSV by these potential vectors was not examined.

TSV is considered endemic in countries along the Pacific coast, ranging from northern Peru up through Mexico (Brock *et al*., 1995, 1997; Hasson *et al*., 1999a; Lightner, 1995, 1996a,b; Zarain-Herzberg and Ascencio-Valle, 2001). Acute and/or chronic disease has been detected in wild *P. vannamei* postlarvae collected in Ecuador and in broodstock captured off of Honduras, El Salvador, and southern Mexico (Brock *et al*., 1997; Lightner, 1995, 1996a,b). Hence, wild postlarvae and broodstock of unknown health history are potential TSV vectors, should be avoided by shrimp growers, and represent another means by which the virus can be transmitted either locally or between countries.

The movement of TSV between countries has mainly been attributed to the sale and export of live postlarvae and adult shrimp with acute or chronic TSV infections (Brock *et al*., 1997; Hasson *et al*., 1999a; Lightner, 1995, 1996a,b, 1999; Lightner *et al*., 1997b). This is the principal means by which TSV was introduced into shrimp farming nations within the Western Hemisphere during 1992 to 1996 and the manner by which the disease entered Taiwan in 1998 (Hasson *et al*., 1999a; Tu *et al*., 1999; Yu *et al*., 2000). The ability of TSV to withstand long-term freezing without loss of infectivity makes frozen shrimp another potential vector of this disease (Hasson *et al*., 1995; Lightner, 1995). Thus, virus spread between countries can occur if a frozen infected product is used as bait for fishing (Lightner, 1995; Prior *et al*., 2001) or if shrimp processing plant wastes are carelessly introduced into local water ways (Lightner, 1995; Lightner *et al*., 1996b, 1997b).

The principal penaeid host of TSV is *P. vannamei*, which is the predominant marine penaeid species farmed in the Americas and which has been introduced into Asia (Jory, 1995; Tu *et al*., 1999). TSV causes serious disease in postlarval, juvenile, and adult shrimp of this species, but has not been reported in *P. vannamei* smaller than those in the postlarval (PL) 11 stage (Brock *et al*., 1995; Lightner, 1996a; Lightner *et al*., 1995, 1997a; Lotz, 1997). The American penaeids *P. stylirostris, P. schmitti, P. setiferus, P. duorarum*, and *P. aztecus* can also be infected by TSV. However, serious acute TSV infections have only been reported for the PL and juvenile stages of *P. setiferus* (Overstreet *et al*., 1997), juvenile stages of *P. schmitti* (Brock *et al*., 1997; Lightner, 1996a) and, most recently, in postlarval and juvenile *P. stylirostris* (Erickson *et al*., 2002; Robles-Sikisaka *et al*., 2002). Findings of TSV-tolerant *P. setiferus* juveniles suggest that different strains of this species are more TSV resistant than others (Erickson *et al*., 1997; Hasson, 1998; Overstreet *et al*., 1997). Similarly, TSV-resistant strains of specific pathogen-free (SPF) *P. vannamei* have been developed through selective breeding

programs initiated and run by the U.S. Marine Shrimp Farming Consortium as a strategy to combat this disease (Argue *et al*., 2002; Carr *et al*., 1997; Lightner, 1995). Limited TSV infectivity studies conducted on the Asian penaeid species *P. monodon, P. japonicus*, and *P. chinensis* suggest that all three species are moderately susceptible to the virus as juveniles (Brock *et al*., 1997; Hasson, 1998; Overstreet *et al*., 1997). However, TSV can mutate, and a recently described new strain of TSV was found to cause severe infection-induced losses in populations of farmed *P. stylirostris*, a species that was previously considered TSV-refractive or tolerant. This finding is troubling as it suggests that all species of shrimp currently deemed refractive or resistant to the disease may be infected if additional TSV strains or serotypes emerge (Brock *et al*., 1995; Erickson *et al*., 2002; Robles-Sikisaka *et al*., 2002).

3. Disease Cycle

Initial descriptions of TSV lesion pathogenesis were incomplete and based on routine histological analyses of either naturally infected *P. vannamei* from farms or experimentally infected shrimp obtained from short-term infectivity studies (Brock *et al*., 1995; Hasson *et al*., 1995; Jimenez, 1992; Lightner *et al*., 1994, 1995). The cyclic nature of a TSV infection was later determined through histological and ISH analyses of experimentally infected *P. vannamei* juveniles and found to consist of three overlapping yet clinically and histologically distinct phases. The cycle consists of a per acute to acute phase, a short transition phase, and a long-term chronic phase (Hasson *et al*., 1999b,c). Lotz *et al*. (2003) have divided the disease cycle into five states (uninfected susceptible, prepatently or latently infected, acutely infected, chronically infected, and dead infected shrimp) for the purpose of describing the epizootiology of the disease in mathematical terms. For the purpose of this review, the three phases of TSV infection cycle will be described (Fig. 2).

The clinical signs of an acute phase infection were described earlier. During this period, beginning as early as 24 h postexposure and lasting between 7 to 10 days, virus-induced mortalities peak, and the infected population suffers its highest losses as shown in Fig. 2, phase 1 (Hasson *et al*., 1999b; Lotz *et al*., 2003). The predominant cell type targeted by TSV is the cuticular epithelium of the foregut, gills, appendages, hindgut, and general body cuticle (Brock *et al*., 1995; Hasson *et al*., 1995; Jimenez, 1992; Lightner, 1995, 1996a; Lightner *et al*., 1994, 1995). Lesions may extend into underlying subcuticular connective tissue and striated muscle (Brock *et al*., 1995; Hasson *et al*., 1995, 1999b; Lightner *et al*., 1994, 1995). In severe cases, the antennal

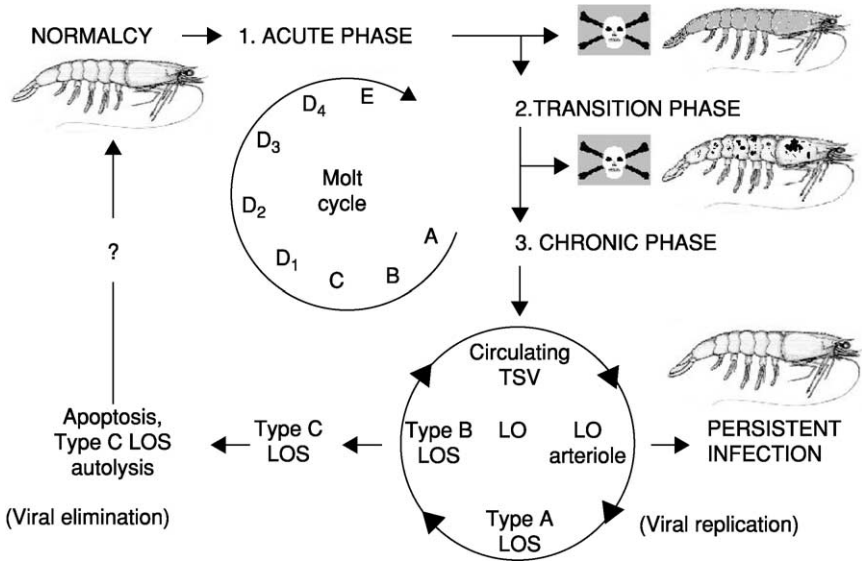

FIG 2. Hypothesized TSV disease cycle in juvenile *Penaeus vannamei* (Phase 1: The acute phase infection targets the cuticular epithelium and subcutis, killing about 60–95% of susceptible shrimp that typically die in preecdysis or postecdysis (stages D_4 or E) and display marked chromatophore expansion. Phase 2: Acute phase survivors enter the transition phase, which is characterized by grossly visible multifocal melanized lesions covering the body, moderate mortality, delay of molt, infrequent acute phase epithelial lesions, sequestering of circulating TSV by hemocytes within the walls of lymphoid organ (LO) arterioles, and interstitial LO spheroid formation. Phase 3: The chronic phase infection begins following molt (postecdysis, stage A) with marked LO spheroid development and LO hypertrophy, with a cessation of mortalities and a return of normal behavior and appearance. Pinocytosis of circulating TSV virions by hemocytes initiates LO spheroid production and morphogenesis beginning with the type A morphotype. Viral replication within the type A LO spheroid produces the vacuolated and necrotic type B form with release of TSV back into the circulatory system, reinitiating spheroid production within the LO and resulting in a persistent chronic infection. Alternatively, the type B spheroid hemocytes may undergo apoptosis and transform into the type C morphotype, resulting in viral elimination with the possibility of the shrimp host returning to a TSV-free state (normalcy). The final outcome of a TSV infection (viral persistence versus elimination) is believed to be largely dependent on the immunological, nutritional, and overall health status of the shrimp. Disease cycle is adapted from Hasson *et al.* (1999b,c); molt cycle adapted from Roer and Dillaman (1993).

gland, hematopoietic tissue, testes, and ovaries may also be infected (Hasson *et al.*, 1999b; Verlee Breland, GCRL, personal communication, 1997). Acutely infected epithelial cells detach from the underlying stroma and assume a spherical shape; cell lysis follows with the liberation of virions into the circulatory system (Hasson, 1998; Hasson *et al.*,

1999b). Histologically, TSV induces a distinctive acute phase lesion consisting of necrotic epithelial cells that display highly basophilic pyknotic and karyorrhectic nuclei, marked cytoplasmic eosinophilia, and variably staining and sized cytoplasmic inclusion bodies (Brock *et al*., 1995; Hasson *et al*., 1995, 1999b; Jimenez, 1992; Lightner, 1994, 1995; Lightner *et al*., 1995). Collectively, these characteristics produce the aptly termed "peppered" or "buckshot laden" appearing histological lesion, which is considered pathognomonic for an acute phase TSV infection (Fig. 3A) (Brock *et al*., 1995; Hasson *et al*., 1995, 1999b; Jimenez, 1992; Lightner, 1994, 1995; Lightner *et al*., 1995). Infection and lysis of the cuticular epithelium does not elicit an immediate

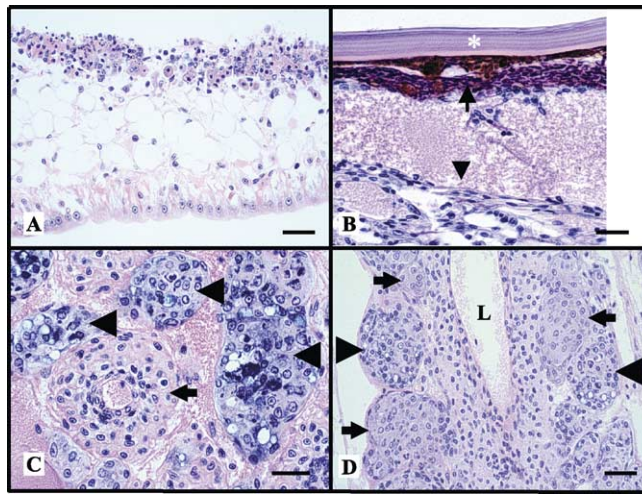

FIG 3. Photomicrographs of naturally occurring acute, transition, and chronic phase TSV infections in *Penaeus vannamei* by routine histology. (A) Head appendage illustrating a pathognomonic severe segmental acute phase TSV infection of the cuticular epithelium and subcutis (Top). The "peppered" appearance of the lesion is principally due to nuclear pyknosis, karyorrhexsis, and karyolysis. Normal uninfected epithelium is present for comparison (Bottom). The surrounding cuticle is absent due to sectioning artifact. (B) A transition phase TSV lesion within the region of the cuticular epithelium and subcuticular connective tissue of a tail segment. A layer of melanized (brown) hemocytic infiltrates (small arrow), located immediately below the exocuticle (*), has replaced the virus-killed epithelium. Edema and fibrous tissue are evident (large arrow head), further indicative of ongoing wound repair. (C) High magnification of the lymphoid organ of a chronically infected shrimp showing a normal arteriole in cross-section (small arrow) and three basophilic type B spheroids (large arrow heads). (D) Type A (small arrow) and type B (large arrow head) spheroids bordering the walls of the subgastric artery in the same shrimp described in Fig. 3C. L = Lumen. Hematoxylin and eosin stain. Bar = 30 μm.

inflammatory response and typically occurs in late premolt or early postmolt stages in *P. vannamei* (Brock *et al.*, 1995; Hasson *et al.*, 1995, 1997, 1999a,b; Lightner, 1996a; Lightner *et al.*, 1994, 1995). Dead shrimp with partially sloughed cuticles are commonly observed during this phase. It is possible that the combined porosity of the cuticle and increased metabolic activity of the epithelium that occurs just prior to and during ecdysis results in increased virus accessibility to epithelial cells whose activated state makes them conductive to viral replication (Hasson, 1998).

Shrimp surviving the acute phase infection enter a brief transitional phase, as shown in Fig. 2 as phase 2, which shares characteristics of both the acute and chronic phases and effectively links them together (Hasson *et al.*, 1999b). The transition phase is characterized by declining mortalities and marked by grossly visible multifocal melanized lesions of the cephalothorax and tail. The histological characteristics include infrequent scattered acute phase epithelial lesions, normal appearing lymphoid organ (LO) arterioles (tubules) that display a diffuse TSV probe positive signal by *in situ* hybridization (ISH), and the initiation of spheroid development within the LO. The grossly visible melanized lesions within the cuticular epithelium consist of hemocytic infiltrates and represent foci of resolving acute phase lesions (Fig. 3B). *P. vannamei* with transition phase infections are grossly and histologically detectable in experimentally infected stocks about 4 days following *per os* exposure to TSV, and this phase has a duration of about 5 days. Transition phase shrimp are lethargic and anorexic, presumably because all resources are devoted to wound repair and recovery. The end of the transition phase and initiation of the chronic phase infection is signaled by resumption of the molt cycle and the shedding of the melanized exoskeleton (Hasson *et al.*, 1995, 1999b,c).

A chronic TSV infection, shown in Fig. 2 as phase 3, begins about 6 days postinfection and was found to have a minimum duration of 8 to 12 months in experimentally infected *P. vannamei* (Hasson, 1998; Hasson *et al.*, 1999c; Jeff Lotz, personal communication, 1997). The characteristics of a chronic TSV infection include a cessation of mortalities, absence of disease signs, and resumption of normal feeding and swimming behavior. Histologically, the hallmark of a chronic TSV infection is the presence of numerous spheroids located within both the interstices of a hypertrophied lymphoid organ and along the external surface of the subgastric artery (Fig. 3C and D). Infrequent numbers of ectopic spheroids are also found associated with tegmental glands located within connective tissues of the cephalothorax and appendages. Spheroids consist of phagocytic semigranular and granular hemocytes

with a high apoptotic index (Anggraeni and Owens, 2000). Routine histology and ISH analyses were used to track the development of spheroids in time-course sampled *P. vannamei* juveniles with experimentally induced chronic TSV infections during a 12-month study (Hasson *et al.*, 1999c). To summarize briefly, spheroid development begins during the transition phase following active pinocytosis and sequestering of circulating TSV particles by resident or transient phagocytic hemocytes located in the walls of the LO arterioles. These activated hemocytes are believed to migrate into the LO interstitium where they form aggregates with other TSV-activated hemocytes. The resulting spheroid is characterized by a well-delineated, lightly basophilic, and variably sized and shaped solid mass of hemocytes. Furthermore, spheroids undergo successive morphological changes and produce three distinct forms that were named morphotypes A, B, and C. The first LO spheroid morphotype to appear, type A, consists of a homogenous mass of hemocytes that is, typically, TSV negative by ISH analysis, presumably containing undetectable levels of virus. The subsequent morphotype to develop, type B, displays multifocal cytoplasmic vacuolization and moderate to numerous necrotic foci that are consistently TSV positive by ISH, indicating ongoing viral replication. The terminal morphotype, type C, displays morphological characteristics of apoptotic cells that are TSV negative by ISH and eventually disappear through combined autolysis and resorption. Continued replication of TSV in type B spheroids with concurrent release of the virus into the shrimp circulatory system perpetuates spheroid production in the LO in a cyclic fashion and induces a persistent infection as shown in Fig. 2, phase 3. In contrast, the progressive transformation of the type B to the type C morphotype, with resultant TSV elimination by apoptosis, could return the shrimp host to a TSV-free state (normalcy). Based on these results and published information on LO physiology, Hasson *et al.* (1999c) proposed that spheroid development in marine shrimp represents a cell-mediated immune response as first suggested by Kondo *et al.* (1994). Further, the function of the LO is to remove biotic and abiotic substances from the hemolymph of the shrimp host that are otherwise too small to illicit an encapsulation response (Hasson *et al.*, 1999c). This same hypothesis has been advanced and supported by more recent studies involving the effects of both viral and bacterial infections on the LO (Anggraeni *et al.*, 2000; Soowannayan *et al.*, 2002; van de Braak *et al.*, 2002). The possible outcomes of a chronic TSV infection include a return to normalcy through the complete elimination of TSV via apoptosis or persistence of a chronic state infection due to continued viral replication. Which of these two

competing processes will prevail within the LO probably depends on the nutritional, immunological, and overall health status of the host (Hasson, 1998; Hasson *et al.*, 1999c).

C. Physical Properties of Taura Syndrome Virus

Initial isolation and characterization work was conducted on sucrose and cesium chloride gradient-purified TSV isolated from *P. vannamei* originating from naturally occurring epizootics in Ecuador (1993) and Hawaii (1994) by Hasson *et al.* (1995). These isolates were found to have icosahedral symmetry (Fig. 4), had a diameter of 31–32 nm and a buoyant density of 1.337 g/ml, were nonenveloped, and replicated within the cytoplasm of host cells. These characteristics suggested that TSV corresponded to either Nodaviridae or Picornaviridae. Subsequent work by Bonami *et al.* (1997) demonstrated that TSV possesses a linear positive-sense ssRNA genome of about 9kb, three major (55, 40, and 24 kDa) and one minor (58 kDa) polypeptides composing the capsid, and an extracted genomic RNA that is itself

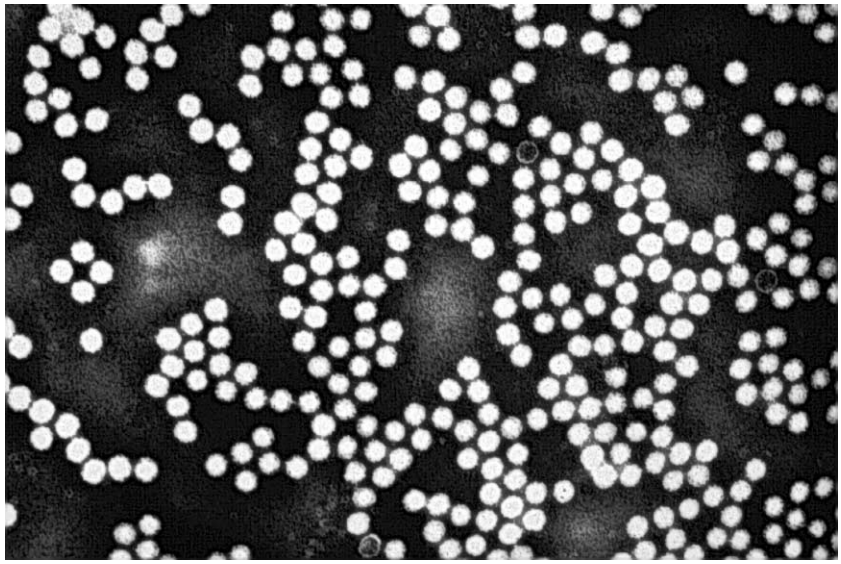

FIG 4. Transmission electron micrograph illustrating CsCl gradient-purified and negatively stained (with 2% PTA) TSV particles isolated from farmed *Penaeus vannamei* originating from Ecuador. The icosahedral viral particles are 31 to 32 nm in diameter and are nonenveloped.

infectious. This latter finding was suggestive of a genome with a polyadenylated 3′-end and the ability to act as a polycistronic mRNA. Collectively, these characteristics justified the classification of TSV as a *Picornavirus* and similarities to insect picornaviruses were discussed by Bonami *et al.* (1997). Subsequent sequence analysis of a cloned segment of the 3′-end of the TSV genome (3728 bp) by Robles-Sikisaka *et al.* (2001) provided further molecular evidence that TSV is similar to other insect picornaviruses. Work conducted by Mari *et al.* (2002) determined the complete sequence of the TSV genome (10,205 nucleotides) and classified the virus as a member of a newly designated group, cricket paralysis-like viruses, in Picornaviridae (van Regenmortel *et al.*, 2000). This group of insect viruses, together with TSV, share similarities with the picornaviruses but are sufficiently different to be grouped separately (Mari *et al.*, 2002).

D. Genome Organization and Gene Expression of Taura Syndrome Virus

The TSV genome comprises a single-stranded RNA of positive polarity with a 3′-poly(A) tail (Bonami *et al.*, 1997). The genome is 10,205 nucleotides (nt) long with a 5′-untranslated region of 377 nt and a 3′-untranslated region of 226 nt (Mari *et al.*, 2002). There are two open reading frames (ORFs) in the TSV genome. ORF1 is 6324 nt long and encodes a 2107 amino acid (aa) polyprotein with a molecular mass of 234 kDa. ORF2 is 3036 nt long and encodes a 1011 aa polypeptide with a molecular mass of 112 kDa (Mari *et al.*, 2002). There is an intergenic region of 226 nt between the two ORFs. ORF1 encodes nonstructural proteins, and ORF2 encodes the virion structural proteins (Mari *et al.*, 2002; Robles-Sikisaka *et al.*, 2001). The ORF1 nonstructural proteins contain sequence motifs that correspond to the conserved motifs of a helicase (NTP-binding protein), a protease, and a RNA-dependent RNA polymerase (RdRp) (Fig. 5). The RNA helicase consensus sequence, Gx_4GK, is present at ORF1 amino acid positions 752 to 758, and the TSV helicase domain shows significant similarity with the cognate domain of insect picorna-like viruses (*Drosophila* C virus, DCV; *Rhophalosiphum padi* virus, RhPV; *Plautia stali* intestinal virus, PSIV; black queen cell virus, BQCV; *Triatoma* virus of the fungus *Triatoma infestans*, TrV; and *Himetobi* P virus, HiPV). The protease domain in the TSV ORF1-encoded polypeptide resides between amino acid residues 1380 to 1570. It also shows similarity with the 3C protease of insect picorna-like viruses as well as other positive-sense RNA viruses of the Picornaviridae, Sequiviridae, and Comoviridae that

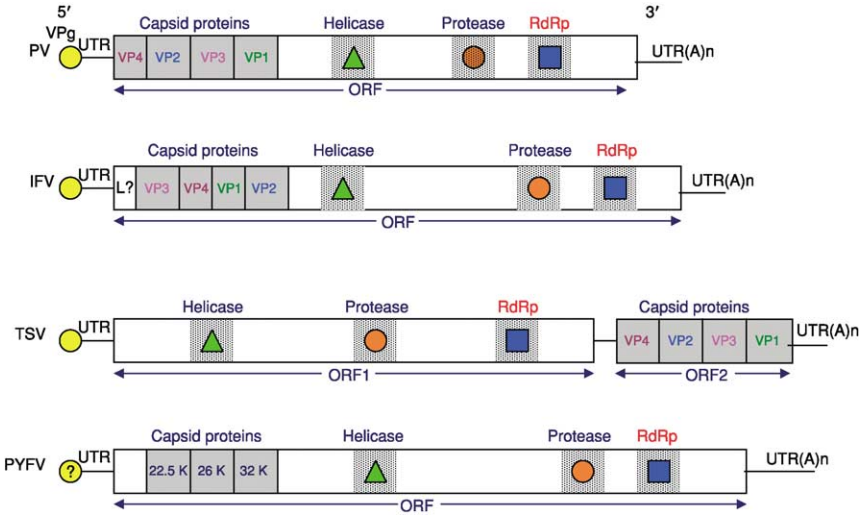

FIG 5. A schematic representation of the genome organization of mammalian and insect picornaviruses and plant RNA viruses. ORF = Open reading frame, UTR = Untranslated region, VPg = Genome linked protein, and ? = The unconfirmed presence of VPg. The helicase (△), protease (○), and the RNA-dependent RNA polymerase (■) regions are indicated.

have a conserved (GxCG) protease motif (Gorbalenya *et al.*, 1989). In TSV, the protease motif is partially conserved with Gly being replaced by Cys. However, like other picornaviruses, the His-Asp-Cys catalytic triad in the protease domain is conserved in TSV (Mari *et al.*, 2002).

The C-terminal region of TSV ORF1 contains the RdRp domain. Multiple alignment of the TSV RdRp domain with homologous domains of other positive-sense RNA viruses is shown in Fig. 6. There are eight conserved motifs in the RdRp (Koonin, 1991) preserved in all insect picorna-like viruses along with picornaviruses of mammalian and plant origin (Fig. 5). Among these, motifs 1, 5, 6, and 7 are more conserved than other motifs, and it has been suggested that these highly conserved motifs might constitute sites for RNA binding (Koonin, 1991). Phylogenetic analysis using the Maximum Likelihood method categorizes picornaviruses into two major clusters (Fig. 7). One cluster contains insect and mammalian picornaviruses and the other the plant picornaviruses. In the first cluster, insect picornaviruses possessing a dicistronic genome (see subsequent paragraphs for detail) group together; in this group, TSV clusters with DCV and cricket paralysis virus (CrPV). The second subcluster contains two groups:

one group includes sacbrood virus (SBV) of honeybee and infectious flacherie virus (IFV) of silkworm, the genome organization of which shares more similarities with mammalian than insect picornaviruses, and the other group includes mammalian picornaviruses (Fig. 7).

In addition to helicase, protease, and RdRp motifs, the TSV genome contains a short aa sequence at the N-terminal end of ORF1 (positions 166 to 230) that shows significant similarity with the inhibition of apoptosis (IAP) proteins found in mammals, yeast, insects, and some DNA viruses (Mari *et al.*, 2002). No other RNA viruses are known to contain such an IAP motif. TSV-infected shrimp that survive the initial acute infection enter into a long-term chronic phase infection (Fig. 2) (Hasson *et al.*, 1999b,c). It remains to be seen if the TSV-encoded peptides containing the IAP motif play any role in evading the host immune system, thus enabling the virus to replicate during the long-term chronic phase infection.

TSV ORF2 contains the capsid proteins. TSV virions contain three major proteins designated as VP1 to VP3 (55, 40, and 24 kDa) and one minor protein (58 kDa) designated as VP0, polypeptide (Bonami *et al.*, 1997). The N termini of VP1 to VP3 have been sequenced, and the order of these proteins in ORF2 was found to be VP2, VP1, and VP3 (Mari *et al.*, 2002). The N-terminal sequence of VP0 has not been determined, and it has been hypothesized that it might be processed from ORF2 in a manner similar to PSIV, an insect picorna-like virus infecting the brown-winged green bug (*Plautia stali*) (Sasaki *et al.*, 1998). The five amino acid motif containing the VP2/VP1 cleavage site in TSV is conserved in insect picornaviruses: TSV (GF↓SKD), PSIV (GF↓SKP), DCV (GF↓SKP), and RhPV (GW↓SKP) (Robles-Sikisaka *et al.*, 2001). The presumed VP1 and VP3 cleavage site in TSV (H↓A) is partially conserved with those used by insect picornaviruses Q↓(A,S,V) (Mari *et al.*, 2002).

A BLASTP search using the ORF2 1011 aa sequence of TSV showed 39 to 43% similarity with the cognate ORF of insect picornaviruses including RhPV (213/482 aa overlap, E = $2e^{-24}$), TrV (231/584 aa overlap, E = $2e^{-20}$), DCV (230/581 aa overlap, E = $3e^{-19}$), PSIV (162/402 aa overlap, E = $4e^{-16}$), CrPV (56/136 aa overlap, E = 2e − 04), and HiPV (230/580 aa overlap, E = $1e^{-15}$) (Robles-Sikisaka *et al.*, 2001). These similarities encompass TSV VP1 and VP2 capsid proteins. A multiple alignment of TSV VP1 and VP2 amino acid sequences with the homologous proteins of insect and mammalian picornaviruses is shown in Fig. 8. A small RNA virus infecting aphids (*Acyrthosiphon pisum* virus, APV) (van der Wilk *et al.*, 1997) has recently been reported to have a genome like those of other insect-infecting RNA viruses that contain

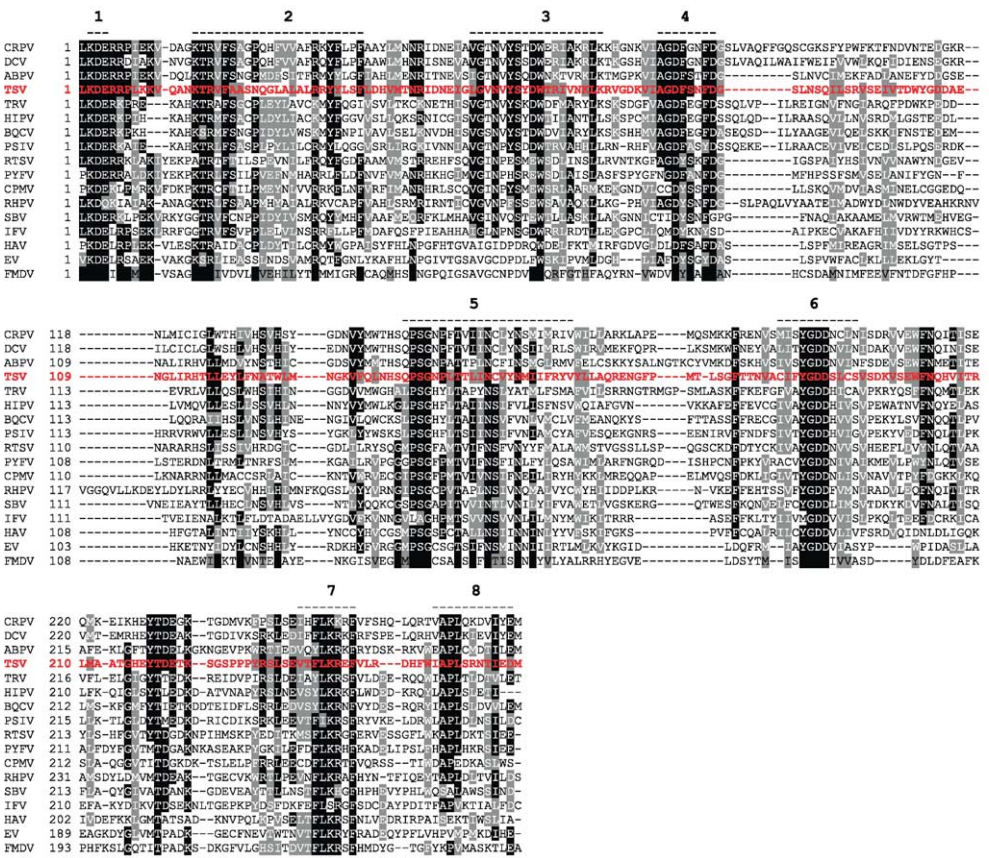
1
2
3
4
5
6
7
8
CRPV
DCV
ABPV
TSV
TRV
HIPV
BQCV
PSIV
RTSV
PYFV
CPMV
RHPV
SBV
IFV
HAV
EV
FMDV

two long ORFs with its virion proteins encoded in the 3′-ORF. The TSV capsid protein sequences, however, show no significant similarity to that of APV.

Northern blot analysis, using total RNA from tail muscle of TSV-infected *P. stylirostris* and radio-labeled probe to a genomic region containing the TSV capsid genes, detected a single transcript of about 10 kb. This suggests that the capsid protein gene is not transcribed as a subgenomic RNA and that the capsid proteins might be translated from the full-length transcript (Robles-Sikisaka *et al.*, 2001). This distinguishes TSV from many positive-stranded RNA viruses (e.g., species of Calciviridae and Togaviridae) in which the capsid proteins encoded in the 3′-end of the genome are generally translated from a subgenomic RNA (Murphy *et al.*, 1995). The TSV transcriptional strategy, however, is similar to insect picornaviruses like RhPV, PSIV, and HiPV, which do not produce a subgenomic RNA for the expression of their capsid proteins encoded in the ORF at the 3′-end of the viral genome.

E. Comparison of Genome Organization of TSV with Insect and Mammalian Picornaviruses

Many picornaviruses have been isolated from a wide range of insect species. Based on their biologic and biophysical properties as well as genome organization data, these viruses were classified as members of a newly designated group, as cricket paralysis-like viruses, in the

FIG 6. Multiple alignment of amino acid sequence of RdRp genes of picornaviruses using the ClustalX program. The alignment is shaded (using up to a 50% consensus) with gray and black indicating similar and identical residues, respectively. The numbers 1 through 8 above the alignment indicate locations of the conserved motifs. A total of 17 *Picornavirus* species were used for the multiple alignment. These include cricket paralysis virus (CrPV; AF218039), Drosophila C virus (DCV; AF014388), acute bee paralysis virus (ABPV; NC002548), *Rhophalosiphum padi* virus (RhPV; AF022937), sacbrood virus (SBV; AF092924), *Plautia stali* intestinal virus (PSIV; AB006531), black queen cell virus (BQCV; AF183905), *Triatoma* virus (TrV; AF178440), himetobi P virus (HiPV; AB017037), infectious flacherie virus (IFV; AB000906), and Taura syndrome virus (TSV; F277675). In addition to insect picornaviruses, the RdRp sequences of the following mammalian picornaviruses were taken for phylogenetic analysis: foot-and-mouth disease virus (FMDV; P03305), human echovirus (EV; AF311938), and hepatitis A virus (HAV; BAA35107). The RdRp sequences of positive-strand RNA viruses infecting plants that were included for the multiple alignment were rice tungro spherical virus (RTSV; A46112), Parsnip yellow fleck virus (PYFV; Q05057), and cowpea mosaic virus (CPMV; P03600).

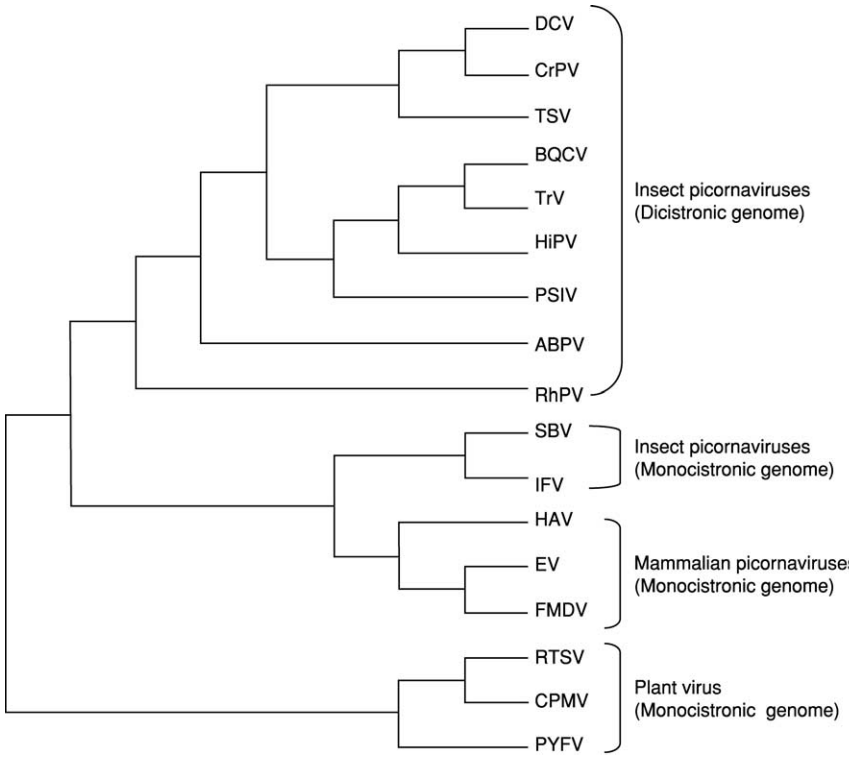

FIG 7. Maximum likelihood phylogenetic tree of picornaviruses infecting insects and mammalian hosts using the amino acid sequence of the RNA-dependent RNA polymerase gene. Plant RNA viruses were used as the out-group. The list of the virus species used for the phylogenetic analysis is the same as used for the multiple alignment of the RdRP gene. The plant picornaviruses were used as an out-group for the phylogenetic analysis. The DNA substitution model used for the analysis was the Hasegawa-Kishino-Yano 85 + I + G; proportion of transitions/transversions was 0.9308; nucleotide frequencies were A = 0.28990, C = 0.19290, G = 0.21940, T = 0.29780; proportion of invariable sites equaled 0.0346; were shape parameter was 2.3891; and the log likelihood of the tree was 15706.94.

family Picornaviridae with CrPV as the type species of this group (Christian and Scotti, 1998; van Regenmortel *et al.*, 2000). Genomes of a number of these viruses have now been sequenced. These include CrPV (AF218039), DCV (AF014388), and acute bee paralysis virus (ABPV, NC002548); BQCV (AF183905), and SBV (AF092924) of honeybees; RhPV (AF022937), PSIV (AB006531), TrV (AF178440), and

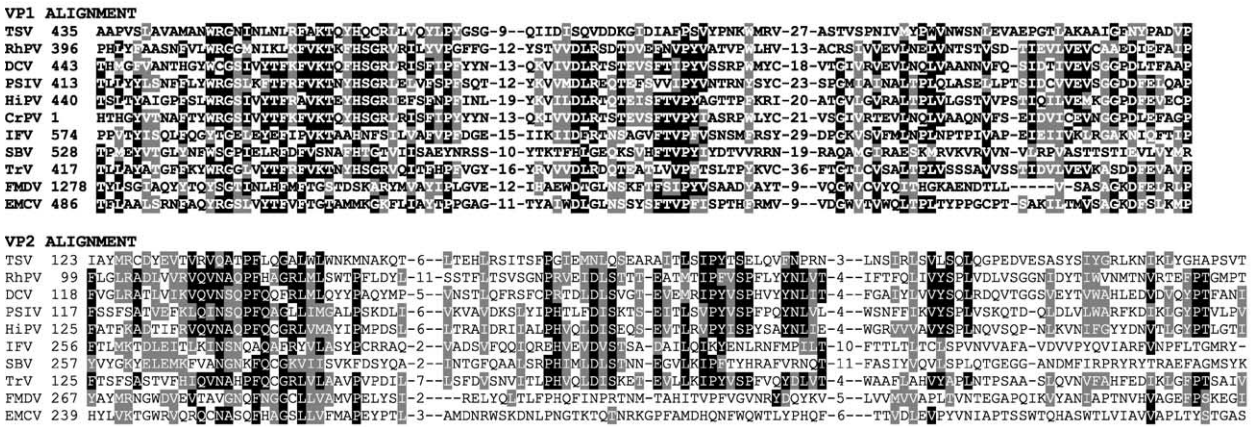

VP1 ALIGNMENT

VP2 ALIGNMENT

FIG 8. Multiple alignment of predicted amino acid sequence of putative VP1 and VP2 capsid proteins of TSV with the homologous proteins of *Rhopalosiphum pisum* virus (RhPV), *Drosophila* C virus (DCV), *Plautia stali* virus (PSIV), *Himetobi* P virus (HiPV), cricket paralysis virus (CrPV), infectious flacherie virus of silkworm (IFV), sacbrood virus of honeybee (SBV), *Triatoma* virus (TrV), foot-and-mouth disease virus (FMDV), and encephalomyocarditis virus (EMCV). For TSV, the amino acid sequence is numbered starting with the N-terminal amino acid of the ORF; for the other viruses, the numbers indicate the starting amino acid position of VP2 or VP. Adapted from Robles-Sikisaka *et al*. (2001) with permission.

HiPV (AB017037); as well as IFV (AB000906) and TSV of shrimp (F277675). Among these viruses, the genome organizations of IFV and SBV were found to be similar to that of mammalian picornaviruses. They contain a single long ORF with the capsid proteins located at the N-terminal end and the nonstructural proteins at the C-terminal end. In contrast, the genomes of CrPV, DCV, RhPV, PSIV, HiPV, TrV, and TSV contain two long ORFs (ORF1 and ORF2) separated by a intergenic region. The 5′-end of ORF1 contains the nonstructural proteins, and the 3′-end of ORF2 contains the capsid proteins (Fig. 5). All of these viruses show greater sequence similarity to each other than with any of the mammalian picornaviruses. In addition, the insect picornaviruses that possess dicistronic genomes have two unique features. First, no subgenomic RNA is produced for translation of the capsid proteins, and second, the coat protein cistron appears to lack an initiating methionine, suggesting that the coat protein is translated through internal initiation and mediated by an internal ribosomal entry site (IRES). Functional IRES elements have been identified in the intergenic region of CrPV and PSIV (Sasaki and Nakashima, 1999; Wilson *et al*., 2000), and cap-independent translation in PSIV ORF2 has been demonstrated *in vitro* using a rabbit reticulocyte lysate (Sasaki and Nakashima, 2000). In CrPV, the initiation codon for IRES-mediated translation was identified as CCU, whereas in PSIV and RhPV, the initiation codon was found to be CUU. It has been shown that the CCU/CUU triplets are part of the inverted repeat sequence of the IRES elements that form RNA psuedo-knot structures essential for IRES activity (Sasaki and Nakashima, 1999; Wilson *et al*., 2000). In TSV, although there is an in-frame methionine in ORF2, N-terminal sequencing of the VP2 capsid protein identified an Ala at the terminal position in the sequenced protein (ANPVEIDNFDTT) (Mari *et al*., 2002). The Ala codon is preceded by both a Pro (CCU) and a Met (AUG) codon (MPANPVE). For Met to be the initiation codon for TSV ORF2, MP residues would need to be removed from the mature protein. Such post-translational processing has never been found in eukaryotes, and it is likely that TSV employs an IRES-mediated cap-independent mechanism for translation of the structural proteins, which is similar to the insect picornaviruses.

In cells infected with insect picornaviruses like DCV, it has been shown that structural proteins are produced in vast excess over nonstructural proteins (Moore *et al*., 1980, 1981). This contrasts to what has been observed in cells infected with human picornavirus, where equimolar amounts of structural and nonstructural proteins are produced

(Ruckert, 1996). The IRES-mediated translation of the coat proteins in insect picornaviruses with dicistronic genomes, therefore, provides a mechanistic explanation for the abundance of structural compared to nonstructural proteins in infected cells. Thus, the translation of the two distinct prolyproteins (ORF1 and ORF2) appears to be independently controlled. This contrasts to the picornaviruses encoding a single ORF in which a single polyprotein is post-translationally processed to generate both the structural and nonstructural proteins (Ruckert, 1996).

F. Genetic Diversity of Taura Syndrome Virus

During the summers of 1999 and 2000, TSV epizootics occurred frequently among *P. stylirostris* shrimp farmed in Mexico. TSV-infected shrimp presented severe acute-phase histological lesions accompanied by high mortality. These shrimp were virus positive by RT-PCR and by ISH but negative by immunohistochemistry (IHC) analyses using a TSV-specific monoclonal antibody (mAb) (Hasson, unpublished data). Severe acute-phase TSV lesions in *P. stylirostris* were observed on only one previous occasion in 1997 in a diagnostic case from Nicaragua (Hasson, unpublished data). Because *P. stylirostris* are characteristically TSV-tolerant, it was speculated that the epizootics in Mexico might have been due to the emergence of a previously unrecognized TSV strain (Hasson, unpublished data). Subsequently, TSV isolates were collected from 16 different farms in Mexico (Sinaloa and Sonora) and then compared with isolates from the United States (Texas and Hawaii), Taiwan, and Nicaragua (Robles-Sikisaka *et al*., 2002). TSV VP1 and VP2 gene regions were amplified by RT-PCR and sequenced. Both VP1 and VP2 coding sequences showed some conservative and nonconservative amino acid replacements among the isolates (Fig. 9). Among these changes, nonconservative replacements of S→A (polar uncharged to nonpolar hydrophobic) in VP1 (Fig. 9A) and Q→K (polar uncharged to positively charged) in VP2 (Fig. 9B) occurred in quite a few isolates. These nonconservative replacements may alter antigenic epitopes involved in antibody binding and contribute to the serological differences identified. Changes in antigenicity and host adaptability resulting from point mutations in the coat protein genes have been reported in mammalian picornaviruses, such as coxsackie virus B4 (Halim and Ramsingh, 2000), encephalomyocarditis virus (Nelsen-Salz *et al*., 1996), human influenza A virus (Fitch *et al*., 1991), and foot-and-mouth disease virus

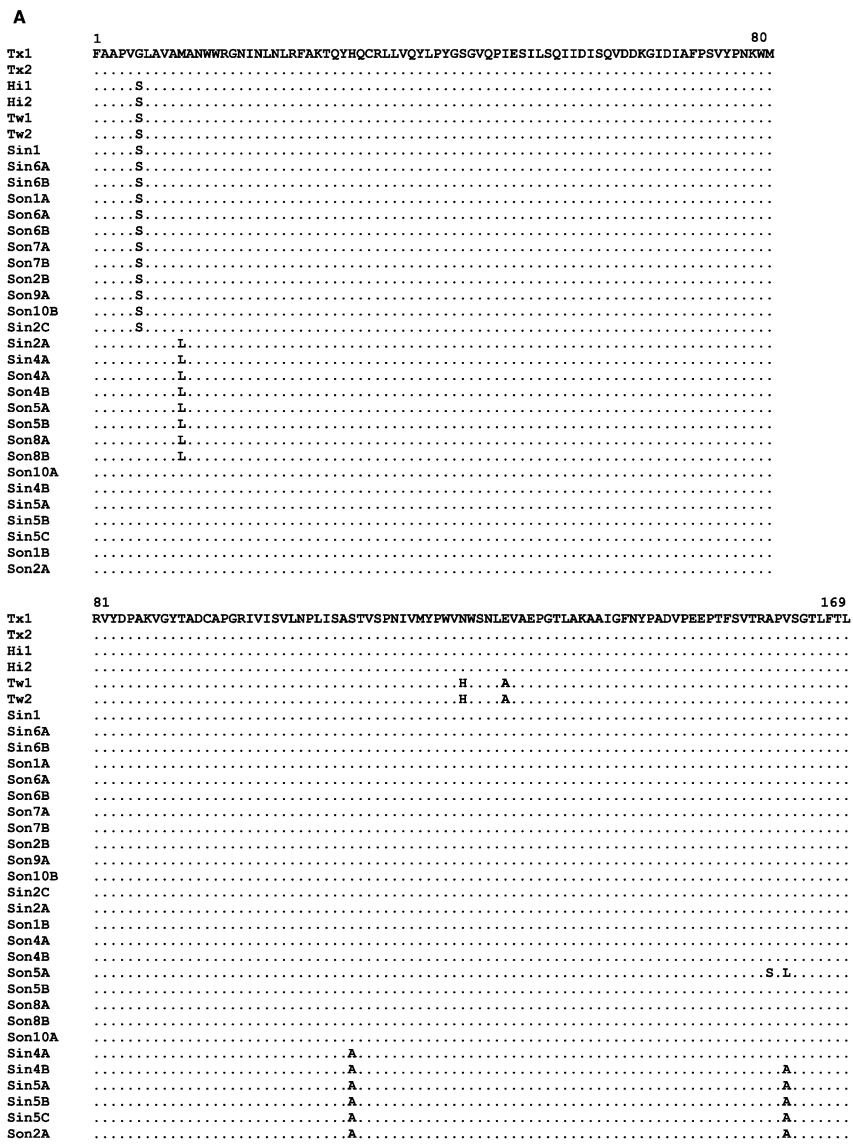

FIG 9. (*continued*)

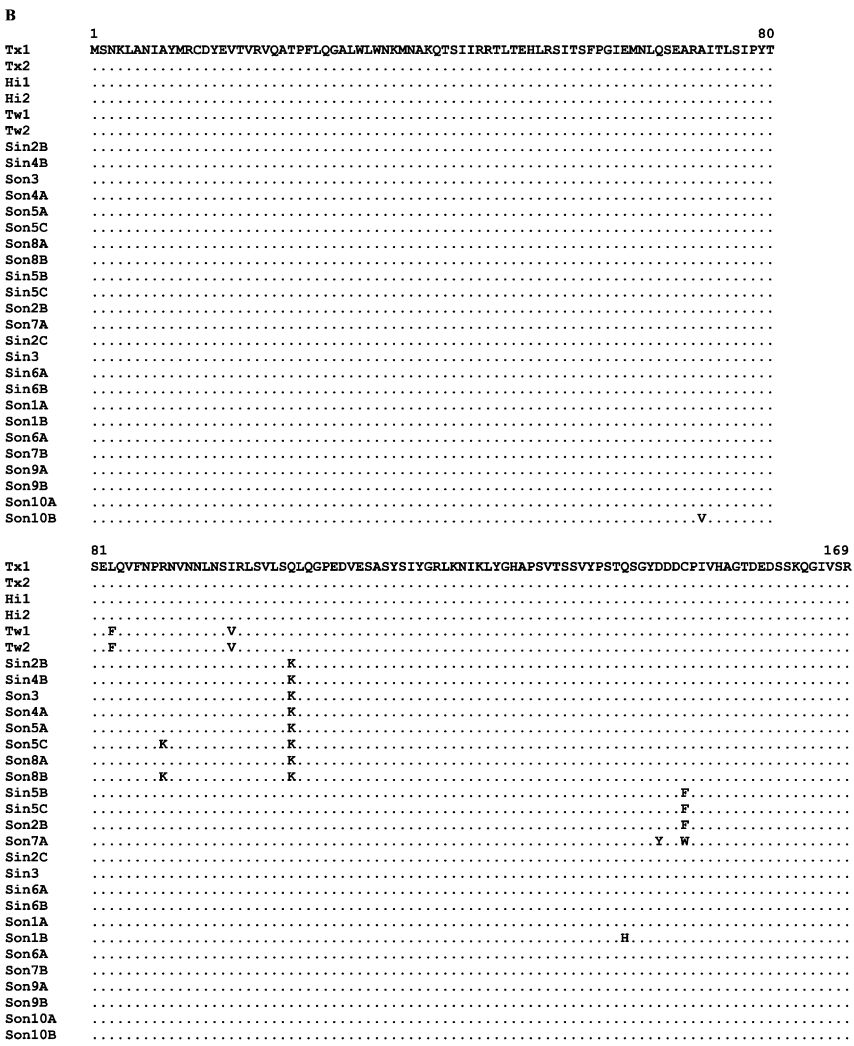

FIG 9. Multiple alignment of predicted amino acid sequences. (A) VP1 sequence. (B) VP2 sequence. Capsid protein genes of TSV isolates were collected from the United States (H_1 = Hawaii, T_x = Texas), Mexico (Son = Sonora, Sin = Sinaloa), and Taiwan (Tw). Identical amino acid is indicated by a dot. Adapted from Robles-Sikisaka *et al.* (2002) with permission.

(Haydon *et al*., 2001; Mateu *et al*., 1988). It remains to be seen if point mutations in VP1 and VP2 genes provide TSV a selective advantage for host adaptability or increased virulence.

TSV-infected shrimp collected from the United States, Taiwan, Mexico, and Nicaragua were analyzed by hematoxylin and eosin-phloxine (H&E) histology and IHC using a TSV-specific mAb. Although all *P. vannamei* and *P. stylirostris* collected from the United States (Texas and Hawaii isolates), Taiwan, Mexico, and Nicaragua showed acute- or chronic-phase TSV infections by H&E histology, IHC produced positive signals with the isolates from Taiwan, Texas, and Hawaii but not the isolates from Mexico and Nicaragua. This suggests that more than one isolate is prevalent in TSV endemic regions (Fig. 10). A similar finding has also been published by Erickson *et al*. (2002). These authors reported that the virus could be detected in all three of their isolates collected from Mexico and from the United States (Hawaii) by Western blot, immuno-dot blot, and IHC analyses using a TSV polyclonal antibody. However, when IHC analyses were conducted using mAb 1A1, only two of three Mexican isolates and the Hawaiian isolate reacted positively, indicating the presence of more than one isolate in TSV epizootic areas. The epitope recognized by mAb 1A1 was putatively localized to the TSV VP1 protein (Erickson *et al*., 2002).

RNA viruses have been found to exist as a mixture of related yet heterogeneous genome sequences (known as "quasi-species") due to lack of effective proofreading activity of RNA polymerase (Domingo and Holland, 1997). Therefore, the existence of TSV strains comprising more than one dominant genotype in infected shrimp populations is not surprising. However, the history of TSV epizootics in Mexico suggests another possibility. When TSV epizootics in Mexico reached a peak in 1996, farmers started switching from culturing TSV-susceptible *P. vannamei* to TSV-resistant *P. stylirostris*. This resulted in the decline of TSV epizootics, and by 1998, shrimp production in Mexico (Sinaloa) appeared to have stabilized (Zarain-Herzberg and Ascencio-Valle, 2001). The replacement of *P. vannamei* with *P. stylirostris* in shrimp farms in Mexico might have contributed to the development of a new strain(s) of TSV as the virus adapted to a new host species. As live postlarvae and adult shrimp are transported from one country to another and across the continents, TSV has spread into new areas where it was not previously present (Tu *et al*., 1999; Yu and Song, 2000). It is, therefore, possible that as naive shrimp populations are exposed to TSV, virus and host selection will evolve, which might result in the emergence of a new and possibly more virulent strain with devastating consequences.

G. Diagnosis of Taura Syndrome Virus

1. Bioassay

TSV infection can be induced by exposing specific pathogen-free (SPF) juvenile shrimp (*P. vannamei*, Kona stock) to TSV-suspect shrimp either by following oral or injection routes (OIE, 2003). Confirmation of TSV presence is then accomplished through analysis of the dying shrimp using histological or molecular methods. The *per os* challenge protocol involves feeding chopped carcasses of suspect shrimp to SPF juveniles in small tanks. TSV-positive indicator shrimp, as identified by gross signs and histopathology, appear within 3 to 4 days post-challenge, and significant mortalities occur within 3 to 8 days. The injection protocol involves homogenizing TSV-suspect shrimp head tissues or whole shrimp in TN buffer or sterile 2% saline solution. Following centrifugation of the homogenate, the clarified supernatant is diluted to 1:10 to 1:100 in sterile 2% saline and filter sterilized, and then 10–20 μl/g body weight is injected intramuscularly into the third tail segment of the shrimp. If the inoculum contains TSV, shrimp begin dying within 1 to 2 days although inocula containing less TSV may take longer to induce mortalities (OIE, 2003).

2. Histological and Immunological Methods

A variety of histological, immunological, and molecular diagnostic techniques are available for the detection of TSV, and these are thoroughly reviewed elsewhere (Lightner, 1996b, 1999; Lightner *et al*., 1998). Routine H&E histology of Davidson's AFA-preserved shrimp tissue (Bell and Lightner, 1988; Humason, 1972) is a standard diagnostic tool used for the identification of TSV-induced pathology. Observation of the pathognomonic acute-phase lesion in cuticular epithelium (Fig. 3A) by light microscopy is sufficient to make a definitive diagnosis of TSV infection (Brock *et al*., 1995, 1997; Hasson *et al*., 1995, 1997, 1999a,b; Lightner, 1995, 1996a,b; Lightner *et al*., 1994, 1995).

An ISH method for detecting TSV in shrimp tissue has been developed that employs two TSV-specific, digoxigenin-labeled cDNA probes (1.3 and 1.5 kb) complementary to the TSV genome (Mari *et al*., 1998). Positive ISH reactions in shrimp histological sections produce a blue–black precipitate within the cytoplasm of TSV-infected cells. One advantage of ISH over routine H&E histology is the greater diagnostic sensitivity, as TSV can be detected in shrimp with mild acute infections that may not be obvious by routine histology. In addition, ISH can

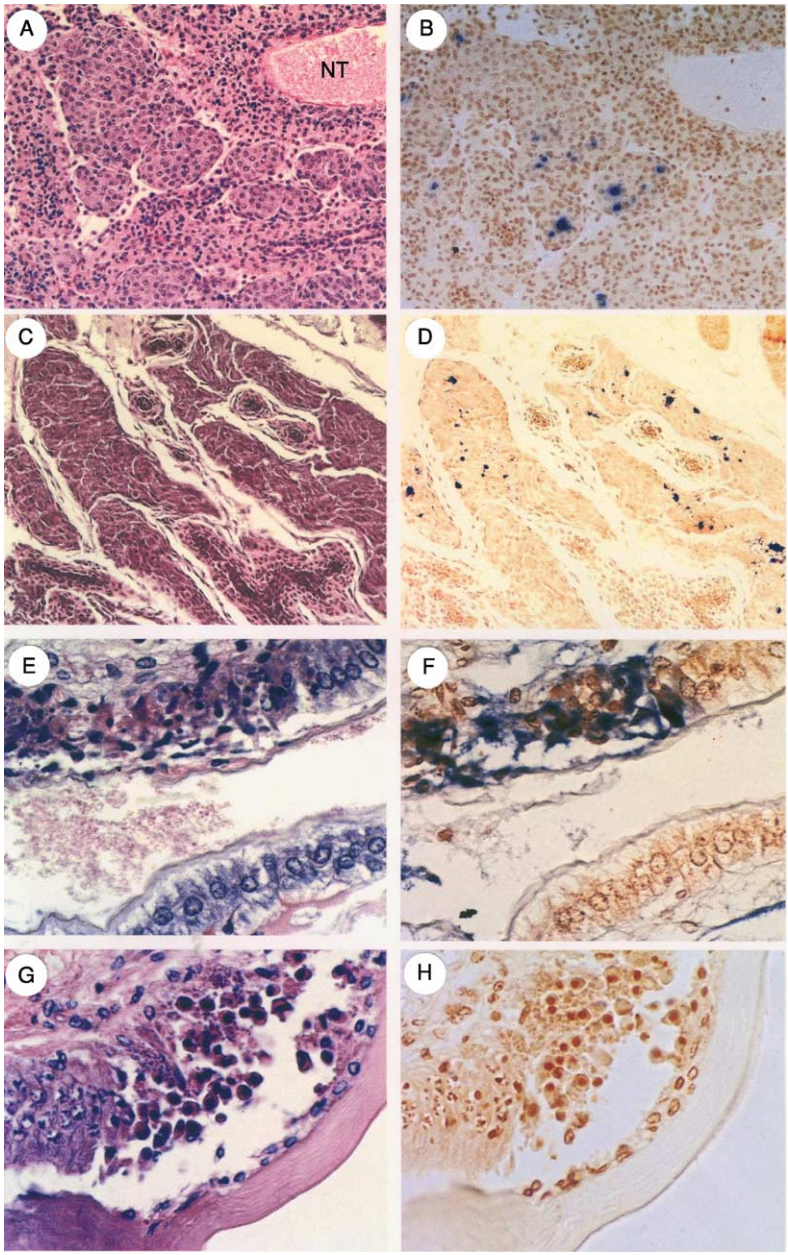

FIG 10. (*continued*)

detect TSV both in asymptomatic and chronically-infected shrimp in which the only histological abnormality is the presence of ectopic or LO spheroids. As LO spheroid development has been associated with at least six different shrimp viral diseases, demonstration of TSV in spheroids by ISH is necessary for a confirmatory diagnosis of this disease (Hasson *et al*., 1999c). Overfixation of TSV-infected shrimp tissue with Davidson's AFA fixative can result in acid hydrolysis of RNA and produce false-negative ISH results. This problem can be avoided by using a fixation time of 24 hr and prompt tissue embedding or preservation in a neutral pH fixative (Hasson *et al*., 1997).

An ELISA-based dot blot test for the detection of TSV capsid protein by use of a TSV-specific monoclonal antibody has been described (Poulos *et al*., 1999), and the procedure has been modified for the IHC detection of TSV in histological sections (Dr. Luis Matheu Wyld, personal communication, 1998). IHC has advantages over ISH in that it is a rapid assay (4 hr versus 36 hr for ISH), more economical, and its TSV detection sensitivity is equivalent to ISH assay. The principle drawback with this technique is that the current commercially available antibody detects the original TSV type strain or isotype but not the Mexican strain identified in *L. stylirostris* (Erickson *et al*., 2002; Robles-Sikisaka *et al*., 2002).

FIG 10. Photomicrographs of consecutive acute or chronic phase TSV-infected tissue sections following analysis by H&E histology (Left column) and immunohistochemistry utilizing a TSV-specific mAb (Right column). (A, B) Lymphoid organ (LO) of a *P. vannamei* juvenile chronically infected with the 1995 Texas TSV isolate. Numerous LO spheroids are located to the left of and below a normal LO tubule (NT) and contain strong multifocal IHC positive signals (blue–black precipitate) (Davidson's fixative, 20X). (C, D) LO of a *P. stylirostris* juvenile submitted by a farm in Taiwan, 2000, and displaying a chronic TSV infection. Small normal LO tubules are surrounded by large, irregularly shaped LO spheroids, that display multifocal IHC positive signals similar to Fig. 10B (Davidson's fixative, 20X). (E, F) Midsaggital section through the anterior stomach of a *P. vannamei* juvenile infected with the 1994 Hawaiin TSV isolate. The upper halves of the photos display a typical acute phase TSV infection of the cuticular epithelium (note pyknotic nuclei), and the lower halves illustrate normal uninfected epithelium. TSV presence in the necrotic region is denoted by the strong IHC signal (R-F fixative, 60X). (G, H) Midsaggital section through the paragnath of a *P. stylirostris* juvenile submitted by a farm in Mexico (Sonora), 2000. The pathodiagnostic acute phase TSV lesion is characterized by nuclear pyknosis, cytoplasmic eosinophilia, and detachment of the infected cuticular epithelial cells from the surrounding matrix in contrast to normal uninfected epithelium located to the far left. IHC analysis produced a negative result denoted by the absence of blue–black precipitate (Davidson's fixative, 60X). Histological sections were stained with H and E. Sections analyzed by IHC were counterstained with Bismarck brown. Adapted from Robles-Sikisaka *et al*. (2002) with permission.

Detection of viruses by their propagation in cell lines is a routine diagnostic tool used in clinical virology laboratories (Lightner and Redman, 1998; Toullec, 1999). A variety of shrimp primary cell cultures have been developed, but an immortalized shrimp cell line has yet to be achieved. As a result, diagnosticians continue to rely on *in vivo* bioassays for shrimp virus detection and amplification (Lightner, 1996a; Lightner and Redman, 1998; Toullec, 1999). A crustacean cell line established from crayfish (*Orconecte limosus*) neuronal cells has been reported (Neumann *et al*., 2000) and is available from the American Type Culture Collection (ATCC). There have been no reported attempts, however, to propagate TSV or other shrimp viruses using this cell line.

3. RT-PCR and Real-Time RT-PCR

An RT-PCR method has been described for the detection of TSV in hemolymph (Nunan *et al*., 1998), and the sequences of primers (9195F and 9992R) used to amplify a 231-bp region of the VP2 gene are given in Table II. Compared to TSV diagnosis based on clinical signs, histopathology and bioassays that are both labor intensive and time consuming, RT-PCR provides a nonlethal diagnostic method that is both rapid and highly sensitive.

Recently, real-time RT-PCR methods using either SYBR Green dye (Dhar *et al*., 2002; Mouillesseaux *et al*., 2003) and the TaqMan probe (Tang *et al*., 2003) have been developed for the rapid detection and quantification of TSV. The real-time PCR assay measures the amplicon accumulation during the exponential phase of the reaction. Amplification profiles and the dissociation curves obtained for a TSV-infected and a healthy shrimp sample together with those obtained for an endogenous shrimp gene, elongation factor-1α, are shown in Fig. 11. The amplification profile indicates a significant increase in fluorescence at 31.25 cycles (recorded as the cycle threshold value [Ct] value) in the TSV-infected sample but not the control sample (Fig. 11A). However, both healthy and TSV infected samples provided equivalent amplification of elongation factor-1α (Fig. 11C). The dissociation curves of the TSV and elongation factor-1α amplicons had peaks at expected temperature, confirming the specificities of these amplicons (Figs 11B and D). The SYBR Green RT-PCR is very sensitive, highly specific, and has a wide dynamic range of detection. It will be very useful for detecting subclinical infection and has a high throughput potential for screening broodstock and other samples for TSV (Dhar *et al*., 2002).

A real-time RT-PCR assay using TaqMan probe has been described by Tang *et al*. (2003). The method is very sensitive and highly specific

in detecting TSV. The high specificity of TaqMan RT-PCR is achieved by the use of a target-specific, dually labeled fluorogenic probe that hybridizes to the template between the PCR primers and is cleaved during polymerase extension by its 5′-exonuclease activity (Holland *et al*., 1991). TaqMan probes, however, are currently quite expensive. Unlike a real-time assay using the TaqMan probe, SYBR Green real-time RT-PCR does not require an additional probe. The diagnostic specificity of SYBR Green real-time RT-PCR is achieved by analyzing the dissociation curve of the target amplicon. However, in TaqMan RT-PCR, both TSV and endogenous shrimp targets can be amplified simultaneously using probes with different fluorogenic tags, which is not possible in SYBR Green RT-PCR.

III. Yellowhead Disease

A. History, Clinical Signs, and Transmission

Yellowhead disease (YHD) syndrome (*Hua leung*) was first observed in 1990 in black tiger shrimp (*Penaeus monodon*) farmed in central Thailand (Limsuwan, 1991). By 1992, the disease had spread to shrimp farming regions on the east and west coasts of the Gulf of Thailand, where YHD has remained enzootic (Boonyaratpalin *et al*., 1993; Limsuwan, 1991). The occurrence and severity of YHD outbreaks in Thailand appeared to diminish following the emergence of white spot syndrome virus (WSSV) in 1994, and yellowhead virus (YHV) or related viruses have since been commonly detected in healthy shrimp (Flegel, 1997; Pasharawipas *et al*., 1997). Although the origins of YHV remain unclear, a review of particle morphology, morphogenesis, and histopathology has suggested that the collapse of the shrimp farming industry in Taiwan in the late 1980s may have been due to YHV rather than *monodon* baculoviruses as had been reported at that time (Chantanachookin *et al*., 1993; Chen and Kou, 1989).

In early descriptions of YHD in Thailand, *P. monodon* with severe signs displayed a pale or bleached body appearance and a yellowish discoloration of the cephalothorax. This latter sign, from which the name YHD is derived, was due to yellowing of the hepatopancreas (HP), which was typically swollen and soft compared to the normal brown HP of healthy shrimp, and due to a yellow–brownish discoloration of gills (Boonyaratpalin *et al*., 1993; Chantanachookin *et al*., 1993; Flegel *et al*., 1995b; Limsuwan, 1991). Juvenile to subadult shrimp were susceptible to YHD, and mortalities were observed to

TABLE II
LIST OF PRIMERS USED FOR THE DETECTION OF TSV, YHV, AND GAV BY CONVENTIONAL AND REAL-TIME RT-PCR

Virus/control gene	Primer	Primer sequence (5′–3′)	Amplicon size (bp)
Conventional RT-PCR:			
TSV	9195F	For: TCAATGAGAGCTTGGTCC	231[a]
	9992R	Rev: AAGTAGACAGCCGCGCTT	
YHV	10F	For: CCGCTAATTTCAAAACTACG	135[b]
	144R	Rev: AAGGTGTTATGTCGAGGAAGT	
YHV	273F	For: CAAGATCTCACGGCAACTCA	273[c]
	273R	Rev: CCGACGAGAGTGTTAGGAGG	
YHV and GAV	GY1	For: GACATCACTCCAGACAACATCTG	794[d]
	GY4	Rev: GTGAAGTCCATGTGTGTGAGACG	
YHV	GY2	For: CATCTGTCCAGAAGGCGTCTATGA	277[e]
	Y3	Rev: ACGCTCTGTGACAAGCATGAAGTT	
GAV	GY2	For: CATCTGTCCAGAAGGCGTCTATGA	406[f]
	G6	Rev: GTAGTAGAGACGAGTGACACCTAT	
Real-time RT-PCR:			
SYBR Green real-time RT-PCR:			
TSV	112F	For: CTGTTTGTAACACTACCTCCTGGAATT	50[g]
	162R	Rev: TGATACAACAACCAGTGGAGGACTAA	
	004F	For: ATGAGAGCTTGGTCCTGGACTTC	78[h]
	081R	Rev: CCCAATCACTAATCAGAATGTAGTGC	

YHV	141F	For: CGTCCCGGCAATTGTGAT	65[i]
	206R	Rev: CCAGTGACGTTCGATGCAATA	
	912F	For: TCAATGAGTTCAATGACGTCGAA	50[j]
	962R	Rev: GAATGGTATCACCGTTCAGTGTCTT	
	399F	For: ATCGGCACAGGAGCAGACA	98[k]
	496R	Rev: GTAACCCCGGCCATGACTT	
Taqman RT-PCR: TSV	1004F	For: TTGGGCACCAAACGACATT	72[l]
	1075R	Rev: GGGAGCTTAAACTGGACACACTGT	
		Probe: CAGCACTGACGCACAATATTCGAGCATC	
Internal control gene:	25F	For: TCGCCGAACTGCTGACCAAGA	55[m]
EF-1 α	79R	Rev: CCGGCTTCCAGTTCCTTACC	

[a] Nunan *et al.* (1998); [b] Wongteerasupaya *et al.* (1997); [c] Tang and Lightner (1999); [d,e,f] Cowley *et al.* (2003); [g,i] Dhar *et al.* (2002); [j,h,k,m] Mouillesseaux *et al.* (2003); [l] Tang *et al.* (2003).

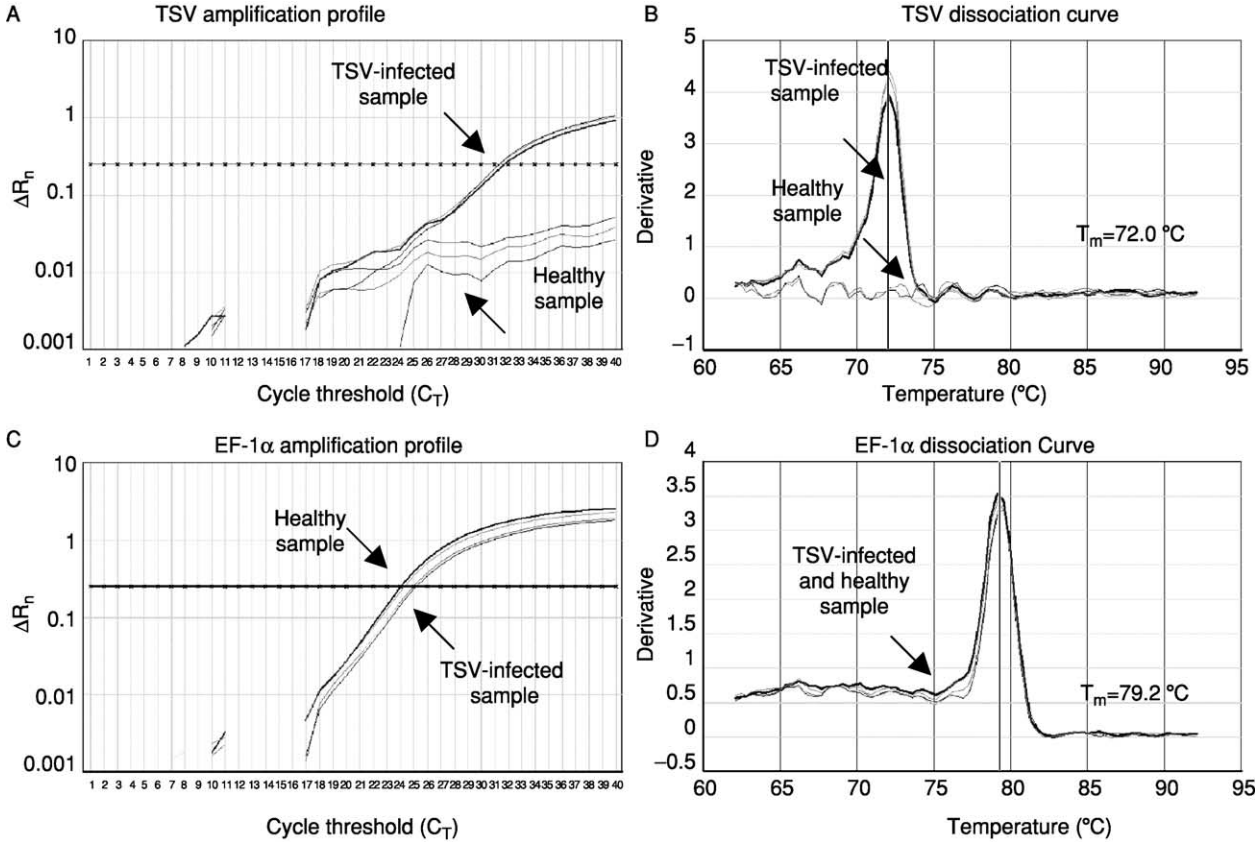

FIG 11. The amplification plots and the corresponding dissociation curves of TSV and EF-1α genes from a TSV-infected shrimp and a healthy shrimp. The melting temperature (Tm) of each amplicon is shown alongside its dissociation curve. Adapted from Dhar *et al*. (2002) with permission.

occur within hours of shrimp displaying clinical symptoms. Original outbreaks were associated with complete pond losses within 3 to 5 days of the first signs of YHD (Limsuwan, 1991). The appearance of gross signs and the congregation of moribund shrimp near the surface at the pond edges were commonly preceded by a period of high-feed consumption followed by an abrupt cessation of feeding (Boonyaratpalin *et al*., 1993; Limsuwan, 1991).

Subsequent to the initial outbreaks in Thailand (Limsuwan, 1991), YHV infection has been reported to occur wherever *P. monodon* is cultured in Southeast Asia and the Indo-Pacific. Countries in which YHV has been reported include China (Lightner, 1996), the Philippines (Albaladejo *et al*., 1998; Natividad *et al*., 1999), Taiwan (Wang and Chang, 2000), Indonesia (Rukyani, 2000), Malaysia (Yang *et al*., 2000), Vietnam (Khoa *et al*., 2000), India (Mohan *et al*., 1998), and Sri Lanka (Siriwardena, 2000). In 1993, a virus morphologically identical to YHV was detected in the lymphoid organs of healthy wild and farmed *P. monodon* in Queensland, Australia, and was given the name lymphoid organ virus (LOV) (Spann *et al*., 1995). In 1995 to 1996 an apparently pathogenic form of this virus was detected in high levels in the gills of moribund farmed *P. monodon* displaying YHD-like histopathology and was named gill-associated virus (GAV) (Spann *et al*., 1997). It is now evident that LOV and GAV represent the same virus observed in chronic and acute phases of infection (Spann *et al*., 2003; Walker *et al*., 2001), and gill-associated virus has become the accepted name for the agent.

The natural occurrence of YHV infections in other penaeid shrimp or crustaceans appears to be uncommon. A yellowhead-like virus has been reported in *Penaeus japonicus* farmed in Taiwan (Wang *et al*., 1996). There is some evidence, based on the transmission of YHD to *P. monodon*, that krill (*Acetes* sp.) and small wild shrimp (*Palaemon styliferus*) from *P. monodon* ponds can carry YHV (Flegel *et al*., 1995b, 1997a). Histopathology consistent with YHV infection was reported in diseased *P. setiferus*, which were also infected with WSSV, at a farm in Texas in 1995 (Lightner *et al*., 1997b). The infections were suspected to have originated from water-borne waste produced at a nearby facility processing *P. monodon* imported from Asia. However, descriptions of YHV infections based on histopathology alone need to be viewed with caution because it has recently been shown that WSSV can cause severe lymphoid organ and connective tissue necrosis in *P. setiferus* and *P. vannamei* that is similar to and can be easily confused for YHV (Pantoja and Lightner, 2003). Apart from one other unconfirmed report of the detection of YHV protein in a *P. setiferus* using an immunoblotting technique (Loh *et al*., 1998), there is no evidence that YHV is

currently present in Western Hemisphere shrimp. Extensive RT-PCR screening of shrimp species indigenous to Australia has identified that GAV is highly prevalent in eastern coast *P. monodon* but, except for some very low-level infections detected in *Penaeus esculentus* that had been cocultivated in a pond with *P. monodon*, is not apparent in other shrimp species (Walker *et al*., 2001).

Experimental transmission studies by feeding or direct injection have shown that YHV has the potential to infect wild shrimp, *Euphasia superba* and *Palaemon setiferus*, commonly found in ponds (Flegel *et al*., 1995a, 1997) and cause disease of varying severity in several species of farmed shrimp. Shrimp species to which YHV can be transmitted include *Penaeus merguiensis* and *Metapenaeus ensis* (Chantanachookin *et al*., 1993), species *Penaeus vannamei* and *Penaeus stylirostris* (Lightner *et al*., 1998; Lu *et al*., 1994, 1997), and species *Penaeus setiferus, Penaeus aztecus*, and *Penaeus duorarum* (Lightner *et al*., 1998) indigenous to the Western Hemisphere. In Australia, GAV has been transmitted experimentally to *Penaeus japonicus, Penaeus esculentus*, and *Penaeus merguiensis* and, as reported for YHV (Lightner *et al*., 1998), species and age affects the severity of disease signs (Spann *et al*., 2000, 2003).

YHV has been transmitted horizontally to *P. monodon* and other species via several routes, including exposure to free water-borne virus particles generated from filtered tissue extracts, cohabitation, and cannibalism of infected carcasses (Flegel *et al*., 1995a; Lightner, 1996; Lightner *et al*., 1998). Transmission by ingestion has been demonstrated from the late postlarval (PL) stages onward. These infectivity studies demonstrated that PL_{20} were quite susceptible, dying 7 to 10 days post-challenge, whereas no mortality occurred in similarly exposed PL_{15} shrimp (Flegel *et al*., 1995b). The ingestion of tissues of *P. monodon* infected with YHV or GAV has proven to be an efficient route of virus transmission to other penaeid shrimp (Lightner *et al*., 1998; Lu *et al*., 1997; Walker *et al*., 2001). Transmission of YHV to *P. monodon* has also been demonstrated by ingestion of infected *Acetes* sp. and *P. styliferus* (Flegel *et al*., 1995a, 1997a).

There is no direct experimental data to demonstrate that YHV is transmitted vertically. It was recognized soon after the first reports of YHD that subclinical carriers might transmit infections to progeny (Chantanachookin *et al*., 1993). Screening of Thai broodstock by electron microscopy, however, identified a low prevalence of YHV infection, which suggested that vertical transmission could not account for the widespread disease (Flegel *et al*., 1997b). There are also no reports of the direct detection of YHV infection in the reproductive organs of

P. monodon broodstock. More recently, a genotypic variant distinct from YHV and GAV has been detected by PCR in high (~55%) prevalence in healthy *P. monodon* PL1-15 postlarvae from hatcheries in Vietnam (Phan, 2001), suggesting that this virus may be perpetuated in farmed stocks by vertical transmission from broodstock. In the case of GAV, there is substantial evidence that vertical transmission contributes to the high (>96%) infection prevalence detected in wild and farmed *P. monodon* from the East Coast of Australia (Cowley *et al.*, 2000a; Spann *et al.*, 1995; Walker *et al.*, 2001). GAV has been detected by RT-PCR in spermatophores and mature ovaries of healthy broodstock and in spermatophore secretions by ISH (Walker *et al.*, 2001), and mature virus particles have been observed by TEM in the spermatophore seminal fluid of adult males reared in captivity (Cowley *et al.*, 2003). Moreover, if one considers the probable ancient origins of GAV (Cowley and Walker, 2002), the origin of progenitor penaeid shrimp dating back more than 500 million years (Siveter *et al.*, 2001) and the limited natural host range, it seems likely that GAV/YHV and other related viruses may have coevolved with *P. monodon*. The maintenance of a subclinical infection state perpetuated via vertical transmission is a common feature of the biology and coevolution of invertebrate viruses.

B. Physical Properties of Yellowhead Virus

Electron microscopy of tissue sections from *P. monodon* displaying YHD clinical signs identified enveloped, bacilliform YHV virions (40–60 nm × 150–200 nm) with rounded ends (Boonyaratpalin *et al.*, 1993; Chantanachookin *et al.*, 1993). Diffuse projections approximately 8 nm thick and 11 nm in length extend from the envelope surface (Wang and Chang, 2000; Wongteerasupaya *et al.*, 1995) (Fig. 12). Negatively stained virus purified from hemolymph in sucrose density gradients display narrowed envelopes extending from particle ends (Wang and Chang, 2000; Wongteerasupaya *et al.*, 1995), and virions with long envelope extensions joined to form doughnut-shaped structures (Nadala *et al.*, 1997a). The origin of these envelope extensions and their role in YHV particle morphogenesis is not clear. Although apparently unique in structure, YHV virions appear to resemble more closely those of toroviruses than other known viruses.

The YHV nucleocapsid has helical symmetry and comprises a coiled filament of 16–30 nm diameter with periodicity of 5–7 nm (Boonyaratpalin *et al.*, 1993; Chantanachookin *et al.*, 1993; Nadala *et al.*, 1997a; Wang and Chang, 2000). Filamentous nucleocapsid precursors approximately 15 nm in diameter and of variable length

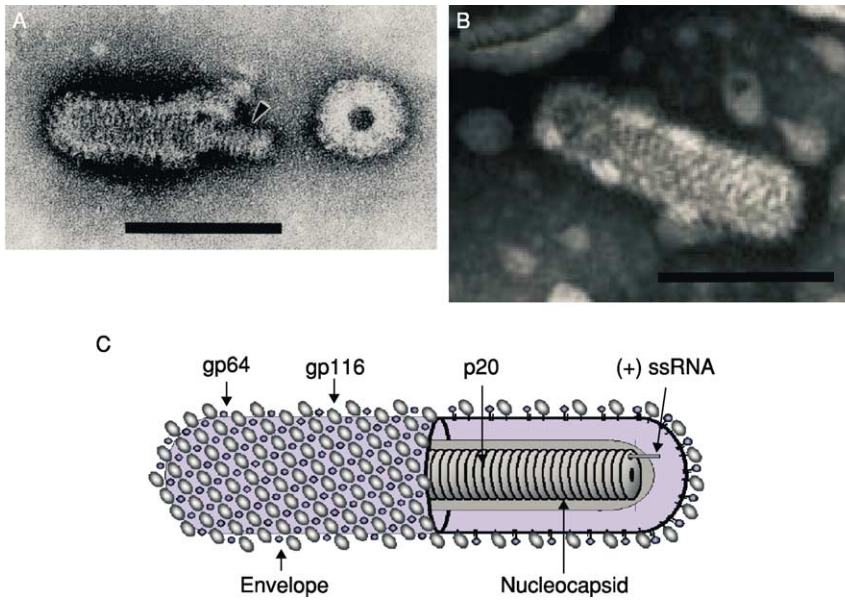

FIG 12. Transmission electron micrographs of negative-stained virions. (A) YHV virion. An arrow highlights the internal nucleocapsid. (B) GAV virion. (C) Schematic illustration of the *Okavirus* virion. Bars a = 100 nm. Electron micrographs (A) From Nadala *et al*. (1997a) and (B) from spann *et al*. (1995); reproduced with permission.

(80–450 nm) occur abundantly in the cytoplasm of infected cells. Nucleocapsids acquire envelopes by intracytoplasmic budding at membranes of the endoplasmic reticulum from which it is presumed the trilaminar lipid envelope of virions is derived. The long nucleocapsid precursors appear to generate elongated enveloped virion precursors that subsequently fragment into discrete rod-shaped virions (Chantanachookin *et al*., 1993). Purified YHV virions paired end to end with an appearance suggesting they may have arisen by fragmentation of longer virions have also been reported (Wongteerasupaya *et al*., 1995). Nucleocapsid precursors and mature enveloped virions are characteristically observed throughout the cytoplasm of infected cells and often within membranous vesicles in which budded virions often align in paracrystalline arrays (Boonyaratpalin *et al*., 1993; Chantanachookin *et al*., 1993). Virions have also been observed near or between the outer and inner nuclear membranes (Chantanachookin *et al*., 1993; Wang and Chang, 2000) in proximity to cytoplasmic nucleocapsid filaments, suggesting that virion maturation can sometimes

occur at these membranes. Virions have also been observed budding from the cytoplasmic membrane (Boonyaratpalin *et al*., 1993), as has also been observed in GAV-infected cells (Spann *et al*., 1995, 1997).

YHV virions have a buoyant density in sucrose of 1.18–1.20 g/ml (Nadala *et al*., 1997a). The lower estimation (1.154–1.162 g/ml) reported by Wang and Chang (2000) appears due to particles not being centrifuged to equilibrium density. Transmission experiments have shown that YHV extracts can remain infectious for at least 72 hr in sea water, and it has been reported that about 30 ppm calcium hypochlorite is an effective disinfectant (Flegel *et al*., 1995b). Other physicochemical properties, including virion pH stability and sensitivity to other chemical agents, have yet to be reported for YHV.

YHV virions purified by sucrose density gradient centrifugation were initially reported to possess three major and one minor structural protein M_r 135, 67, 22 kDa, and 170 kDa, respectively (Nadala *et al*., 1997b). Subsequent analyses employing Coomassie blue rather than silver staining identified only three proteins of M_r 110–116, 63–64, and 20 kDa (Jitrapakdee *et al*., 2003; Wang and Chang, 2000). A method employing sodium metaperiodate oxidization of protein-linked carbohydrate followed by the detection of the oxidized carbohydrates using biotin-linked-hydrazide and streptavidin-horseradish peroxidase has been used to determine the glycosylation status of the virion proteins. Using this approach, Nadala *et al*. (1997b) showed that the 135-kDa protein was glycosylated, and Jitrapakdee *et al*. (2003) subsequently detected carbohydrates in both larger (116 and 64 kDa) proteins. As a low concentration of metaperiodate used at low temperature preferentially oxidizes terminal sialic acid residues, it is possible such residues are more prevalent in the 116–135-kDa protein and that differences in methodology contributed to this discrepancy in carbohydrate detection. Jitrapakdee *et al*. (2003) also employed a thymol-H_2SO_4 carbohydrate detection method dependent on the presence of hexosyl, hexuronosyl, or pentosyl residues (Racusen, 1979) to confirm that both larger YHV virion proteins were glycosylated, and these were designated gp116 and gp64 (Table III).

It is likely the gp116 and gp64 glycoproteins form the projections emanating from the envelope of the virion. However, direct evidence for this using immuno-electron microscopy and monoclonal antibodies (mAbs) generated to semipurified YHV (Sithigorngul *et al*., 2000, 2002) has been obtained only for gp116 (Soowannayan *et al*., 2003). Immunogold labeling with mAb V3-2B, which binds to the gp116 structural glycoprotein in Western blots, deposited gold particles on the envelope periphery of purified virions. Virions were not labeled with mAb Y18

TABLE III
PUTATIVE FUNCTIONS AND PROTEIN SIZE ESTIMATES OF THE YHV STRUCTURAL PROTEINS

Large spike glycoprotein	S1	gp116[a]	110–135 kDa[b]
Small spike glycoprotein	S2	gp64	63–67 kDa
Nucleocapsid protein	N	p20	20–22 kDa

[a] Nomenclature from Jitrapakdee *et al.* (2003).
[b] Apparent M_r values determined by electrophoresis (Jitrapakdee *et al.*, 2003; Nadala *et al.*, 1997a; Sithigorngul *et al.*, 2002; Wang and Chang, 2000).

specific to the gp64 structural glycoprotein, and it may be that the antigenic epitope targeted by this antibody is internal to the protein structure and thus inaccessible. The mAb Y19 specific to the small (20–22 kDa) structural protein also did not bind to intact virions. However, when used on ultra-thin tissue sections, gold particles were observed to bind to free filamentous nucleocapsids in addition to the internal, electron dense, virion nucleocapsids (Soowannayan *et al.*, 2003). The binding of MAb Y19 to nucleocapsids, which would be inaccessible in purified virions, suggests that the nonglycosylated p20 protein is likely to be the virion nucleocapsid protein. The predicted functional roles of the three YHV structural proteins are listed in Table III.

The first report on the nature of the YHV genome isolated from purified virions indicated that it comprised RNA rather than DNA (Wongteerasupaya *et al.*, 1995). This finding contradicted earlier taxonomic descriptions of YHV, based on particle morphology and association with nuclear membranes, as a granulosis-type baculovirus (Boonyaratpalin *et al.*, 1993; Chantanachookin *et al.*, 1993). Nadala *et al.* (1997a) subsequently showed that the YHV genome comprised an unsegmented single-stranded RNA of at least 22 kb. Because no proteins were detected following *in vitro* translation of virion RNA, the genome was tentatively assigned to have negative-sense polarity (Nadala *et al.*, 1997a). However, Tang and Lightner (1999) subsequently isolated RNA from clarified hemolymph presumed to contain mature extracellular virions as a template for cDNA synthesis reactions employing primers of complementary polarities. A PCR product was only obtained for cDNA synthesized using primers that were antisense to a continuous open reading frame (ORF), indicating YHV genomic RNA was likely to be of positive-sense polarity. By *in situ* hybridization (ISH), YHV in shrimp tissues was also only detected using RNA probes synthesized in antisense to ORFs encoded in three independent cDNA clones. However, as the antisense RNA probes would also have

detected YHV mRNA, these data are inconclusive. Subsequent comparisons of genome sequence, organization, and coding strategy have resolved that YHV, like GAV, is most closely related to the (+) RNA viruses of the order Nidovirales (Cowley and Walker, 2002; Cowley *et al*., 2000b, 2001, 2002a; Sittidilokratna *et al*., 2002).

C. Genome Organization and Gene Expression of Yellowhead Virus

The International Committee on Taxonomy of Viruses (ICTV) has recently ratified the classification of YHV, together with GAV as a type species in new genus *Okavirus* of the new family Roniviridae within the Nidovirales (Mayo, 2002; Walker *et al*., 2003). The name *Okavirus* is derived from the observation that the viruses are commonly detected in the shrimp lymphoid or "Oka" organ. Roniviridae (sigla rod-shaped *ni*dovirus) recognizes their distinctive rod-shaped virion morphology (Cowley and Walker, 2002; Cowley *et al*., 2000b; Mayo, 2002). Classification within the Nidovirales was supported by identified phylogenetic relationships between GAV and nidoviruses in the viral replicase genes in the 5′-terminal 20-kb region of the GAV (+) ssRNA genome (Cowley *et al*., 2000b; González *et al*., 2003; Gorbalenya *et al*., 2002). The discovery that GAV synthesizes 3′-coterminal subgenomic (sg) mRNAs (Cowley *et al*., 2002a) consistent with the gene transcription strategy used by coronaviruses, toroviruses, and arteriviruses, also supports taxonomic classification in the Nidovirales.

YHV and GAV possess a (+) sense ssRNA genome that is 3′-polyadenylated (Cowley and Walker, 2002; Cowley *et al*., 2000b; Jitrapakdee *et al*., 2003). Sequences of YHV genome regions encompassing the approximately 8-kb ORF1b (Sittidilokratna *et al*., 2002) and approximately 5-kb ORF3 genes (Jitrapakdee *et al*., 2003) have been reported. Short sequences within the ORF1b gene targeted by RT-PCR tests have also been described (Cowley *et al*., 2000a; Soowannayan *et al*., 2003; Tang and Lightner, 1999; Wongteerasupaya *et al*., 1997). Because the complete sequence of the YHV genome has yet to be reported, known information on gene organization will be described in relation to that determined for the 26,235-nt (+) ssRNA genome of the closely related GAV (Cowley and Walker, 2002, Cowley *et al*., 1999, 2001, 2000b). The GAV genome is organized into 5 ORFs ordered 5′-ORF1a/ORF1b-ORF2-ORF3-ORF4-$[A]_n$-3′ (Cowley and Walker, 2002). The GAV and YHV genome structures are shown in Fig. 13. The details of the intergenic region (IGR) lengths and the lengths and deduced molecular masses of the predicted gene ORFs are listed in Table IV.

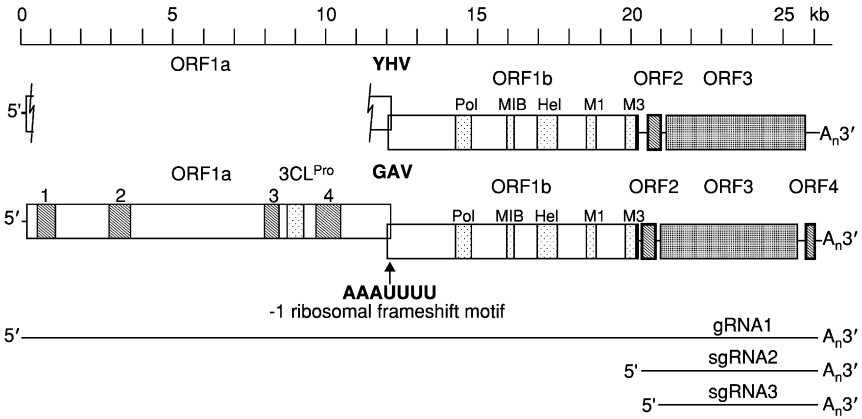

FIG 13. Organization of the complete 26,235 nt (+) ssRNA genome of GAV and the ORF1b and structural genes of YHV. The relative positions of four regions (1–4) containing clusters of hydrophobic residues and the 3C-like proteinase (3CL^{pro}) are indicated in ORF1a in addition to the SDD polymerase (Pol), the three metal ion binding (MIB) domains, helicase (Hel), and motif 1 (M1) and 3 (M3) domains in ORF1b. The AAAUUUU slippery sequence in the ORF1a–1b overlap that precedes an RNA pseudo-knot and is the site of −1 ribosomal frameshifting to generate the pp1ab replicase polyprotein is identified. As ORF4 in GAV is truncated to 20 amino acids in YHV due to an insertion generating a stop codon, this ORF is not indicated in YHV. The full-length gRNA and the two subgenomic (sg)mRNAs with 5′-termini mapping to the intergenic regions upstream of ORF2 and ORF3 of GAV are also shown.

The 5′-terminal 20-kb portion of the GAV genome is occupied by a large replicase gene comprising two long ORFs [ORF1a (12,248 nt) and ORF1b (7942 nt)], which overlap by 99 nt (Cowley *et al.*, 2000b). Although ORF1a continues to the putative 5′-end of the genome, the first inframe putative initiation codon (AUG) resides 68 nt downstream of the 5′-terminal "A" nucleotide determined using a 5′-rapid amplification of cDNA ends (RACE) technique. The putative initiation codon is in a highly favorable context for translation initiation (Kozak, 1986), suggesting that the upstream region is untranslated (Cowley *et al.*, 2000b). The 5′-terminal 152-nt sequence of the YHV genomic RNA has also been determined using the 5′-RACE method (Cowley and Sittidilokratna, unpublished data). In this region, the YHV sequence is 87.5% identical to GAV. The terminal 19 nt are absolutely conserved, and a 3-nt insertion occurs in the putative YHV untranslated region upstream of the ORF1a start codon (Fig. 14). Experimental data have demonstrated that translation of the putative polyprotein pp1ab of

TABLE IV
THE DETAILS OF THE INTERGENIC REGION (IGR) LENGTHS AND THE LENGTHS AND DEDUCED MOLECULAR MASSES OF THE PREDICTED ORFS IN GAV AND YHV GENOMES[a]

	Nucleotide		Amino acid		kDa	
Genome region	GAV	YHV	GAV	YHV	GAV	YHV
5′–genomic UTR	68	71				
ORF1ab–ORF2 IGR						
ORF2–ORF3 IGR	57	54				
ORF3–ORF4 IGR	256	297				
ORF1a			4060	ND[b]	460.3	ND[b]
ORF1b			2646	2618	302.5	299.3
ORF2			144	146	15.9	16.2
ORF3			1640	1666	182.0	185.7
ORF4			83	20	9.6	ND[b]

[a] Information of YHV reproduced from Sittidilokratna (2003) with permission.
[b] ND means not determined.

```
YHV 5′-ACGUUACGUUCCACGUACUAUUCCCACUGCACUCAAUAAACCUUUAUACCCGUUUUCAAU  60
GAV 5'-...................UA..........UCA......U...C---..A......C.G  57
                                  E         L                 L
                     M  E  P  F  Q  V  L  S  L  L  A  T  S  F  S  L
YHV     CGUUACCGACCAUGGAACCUUUUCAGGUUCUAUCGUUGUUGGCAACAUCCUUCAGUCUAC 120
GAV     ....U...........G......G.........U................C.......CU 117
        F
        L  L  L  L  R  I  L  D  R  G  T  T  V  L  S  A  V  R
YHV     UCCUAUUGCUUAGGAUCCUAGACCGCGGCACGACUGUUCUGUCUGCCGUCAGA         173
GAV     ...................C.....U......ACUGUUCUGUCUGCCGUCAGA         170
```

FIG 14. Alignment of the 5′-terminal sequences of the genomic RNA of YHV and GAV determined by sequence analysis of multiple clones generated using a 5′-RACE method (Cowley *et al.*, 2000b). The coding sequence of the predicted N terminus of the pp1ab replicase polyprotein encoded by the ORF1a/1b gene is indicated, and amino acid and nucleotide variations in GAV are shown above and below the YHV sequences, respectively. The region targeted by the 5′-RACE antisense primer is underlined.

GAV is facilitated by a−1 ribosomal frameshift element employing an AAAUUUU "slippery" sequence that immediately precedes a predicted complex RNA pseudo-knot (Cowley *et al.*, 2002a). As shown in Fig. 15 and compared to that of GAV, the −1 ribosomal frameshift element in the ORF1a/ORF1b overlap of YHV has few (11/188 nt = 9.3%) differences, and 3 of 4 nt changes in predicted base-paired sequences are either commensurate or preserve the predicted RNA folding structure

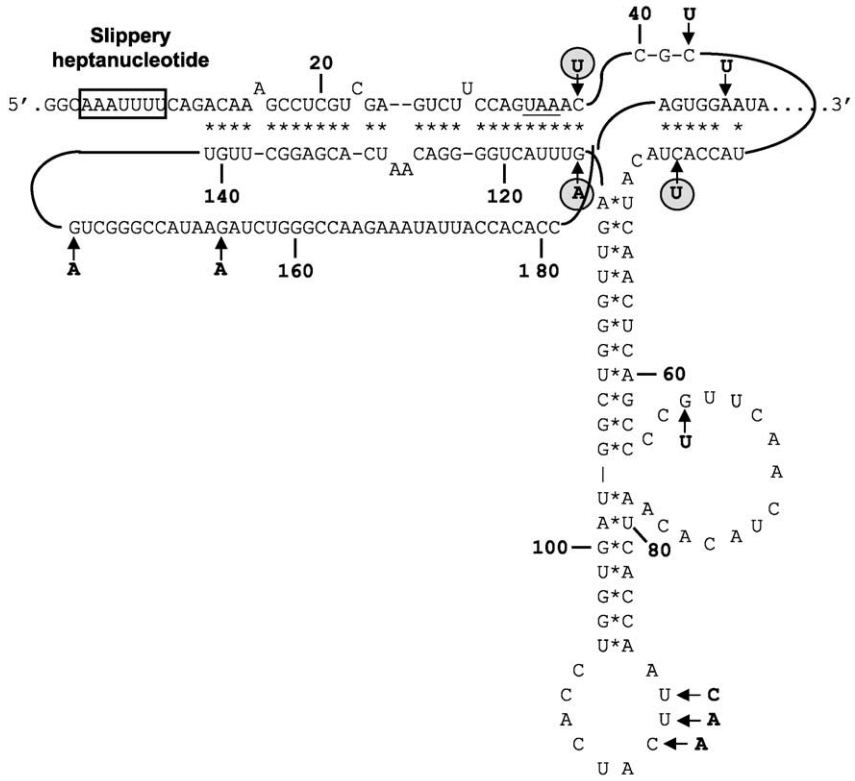

FIG 15. Schematic representation of the −1 ribosomal frameshift site and predicted RNA pseudo-knot in the YHV ORF1a/ORF1b overlap region used for translation of pp1ab replicase polyprotein. Sequence differences to GAV are shown (arrows), and compensatory nucleotide changes that maintain base pairing in the pseudo-knot structure are circled.

(Sittidilokratna *et al*., 2002). Compared to the GAV ORF1b sequence that overlaps ORF1a by 99 nt (33 aa), the YHV ORF1b/ORF1a overlap is trimmed to 36 nt (12 aa) by the presence of a UGA stop codon 3 nt upstream of the AAAUUUU frameshift motif. In both viruses, −1 frameshifting at this motif is predicted to occur at the Phe (F) codon in ORF1a (AAAUUUU) and ORF1b (AAAUUUU) to generate the ORF1a/ORF1b read-through sequence-HEANFSDK- (Cowley *et al*., 2000b; Sittidilokratna *et al*., 2002).

The replicase gene encoding ORF1a (4060 aa) and ORF1b (2646 aa) in GAV can thus generate two polyproteins, pp1a (460 kDa) and a

C-terminally extended pp1ab (759 kDa), likely to be generated in lower abundance as −1 ribosomal frameshifting occurs at about 24% efficiency (Cowley *et al*., 2000b, 2002a). As in other nidoviruses, the pp1ab replicase polyprotein is expected to be involved in genome replication and transcription of the 3′-coterminal sgmRNAs required for efficient translation of the viral structural proteins (Cowley *et al*., 2002a). Sequence analysis of pp1a identified four regions with clusters of hydrophobic residues predicted to contain multiple transmembrane (TM) domains. Hydrophobic regions 3 and 4 (Fig. 13) flank a putative chymotrypsin-like (3C-like) proteinase ($3CL^{pro}$) domain, which was the only pp1a region with detectable similarity to other nidoviruses (Cowley *et al*., 2000b; Ziebuhr *et al*., 2003). A recombinant GAV $3CL^{pro}$ has been shown to cleave at sites in pp1a (^{2827}LVTHE ↓ VRTGN^{2836}) and in the C terminus of pp1ab (^{6441}KVNHE ↓ LYHVA^{6450}), and the tentative consensus sequence VxHE ↓ (L, V) has been proposed (Ziebuhr *et al*., 2003). Several other potential $3CL^{pro}$ cleavage sites in pp1ab with this motif have yet to be confirmed. However, this cleavage site specificity and other structural characteristics defined by the GAV $3CL^{pro}$ sequence indicate that it is distinct from those currently known for mammalian or plant pathogens and bridges an evolutionary gap between the distantly related proteinases of coronaviruses and plant potyviruses (Ziebuhr *et al*., 2003).

Sequence comparison of the 2646 aa ORF1b coding sequence identified homologues of nidovirus RNA-dependent RNA polymerase (RdRp), metal ion binding (MIB), helicase, and the motif 1 and motif 3 (C-terminal) domains (de Vries *et al*., 1997). Although very little similarity occurs elsewhere in the RdRp, the functional domains are shared with the supergroup 1 (+) RNA viruses (Koonin, 1991), and the conserved amino acids are completely preserved in GAV (Cowley *et al*., 2000b) and YHV (Sittidilokratna *et al*., 2002). This includes the SDD, rather than GDD, RdRp core motif, which is unique to nidoviruses. Downstream of the polymerase in YHV and GAV is a cluster of three MIB or zinc finger motifs characteristic of TFIIIA-like fingers (Gorbalenya *et al*., 1989) based on the spacings within each block of four Cys/His residues and on the positioning of surrounding aromatic residues. The helicase domain contains the Pur NTP-binding motifs A (GppGtGKT/S) and B (DE) characteristic of the dsRNA duplex unwinding enzymes of nidoviruses and other RNA viruses (Gorbalenya and Koonin, 1989). Limited homology is also detectable in two domains, described as motifs 1 and 3 in coronaviruses and toroviruses (de Vries *et al*., 1997), between the helicase and C terminus of the ORF1b coding sequence of YHV and GAV (Cowley *et al*., 2000b;

Sittidilokratna *et al.*, 2002). The significance of this will only become apparent when the function of these nidovirus motifs is better understood.

Compared to GAV, the YHV ORF1b sequence contains a 9-nt (3-codon) insertion in the region between the polymerase and metal-ion binding (MIB) domains, a codon deletion downstream of the helicase domain, and a codon insertion immediately preceding the stop codon (Sittidilokratna *et al.*, 2002). Overall, the ORF1b amino acid coding sequences of the two viruses are 88.9% identical. Their sequences in the functional motifs of the RdRp and helicase domains, however, are almost identical, and the putative active Cys and His residues of the three MIB motifs are absolutely preserved. A phylogenetic tree constructed using the ORF1b RNA-dependent RNA polymerase (RdRp) domain of YHV and GAV showing the distant evolutionary relationship of these okaviruses of the Roniviridae to members of the Coronaviridae (coronaviruses and toroviruses) and the Arteriviridae is shown in Fig. 16.

The GAV ORF2 gene encodes a 144-aa (16.0-kDa, pI = 9.75) protein that contains 19 (13%) proline residues and is highly hydrophilic, containing 20 (14%) basic and 13 (9%) acidic amino acids (Cowley *et al.*, 2004b). The 146-aa ORF2 (16.3 kDa) sequence determined for YHV is 83.6% identical and possesses a similar overall charge structure to GAV ORF2 (Sittidilokratna, 2003). Immuno-gold labeling of free and virion encapsidated nucleocapsids of GAV by antibodies to a synthetic ORF2 peptide and a recombinant ORF2 protein indicates that the ORF2 gene product is likely to be the viral nucleocapsid protein (Cowley *et al.*, 2004b). GAV ORF2 antibodies cross-react with the YHV p20 structural protein, and antibodies to YHV p20 have also been shown to bind to nucleocapsids (Soowannayan *et al.*, in press). The genome organization of GAV and YHV is thus distinct from the vertebrate nidoviruses in which the nucleocapsid protein gene resides in the near 3′-terminal genome region downstream of genes encoding the structural glycoproteins and integral membrane (M) protein (de Vries *et al.*, 1997).

The YHV ORF3 gene encodes a 1666-aa (185.7-kDa) protein that contains six highly hydrophobic regions that are likely to be transmembrane domains and has the predicted membrane topology shown in Fig. 17 (Jitrapakdee *et al.*, 2003). The cognate 1640-aa (182-kDa) protein encoded by the GAV ORF3 gene has an identical hydropathic profile (Cowley and Walker, 2002) and overall displays 75% identity to YHV ORF3. The N-terminal sequence analyses have shown that the YHV virion gp116 and gp64 proteins are encoded in the ORF3 gene

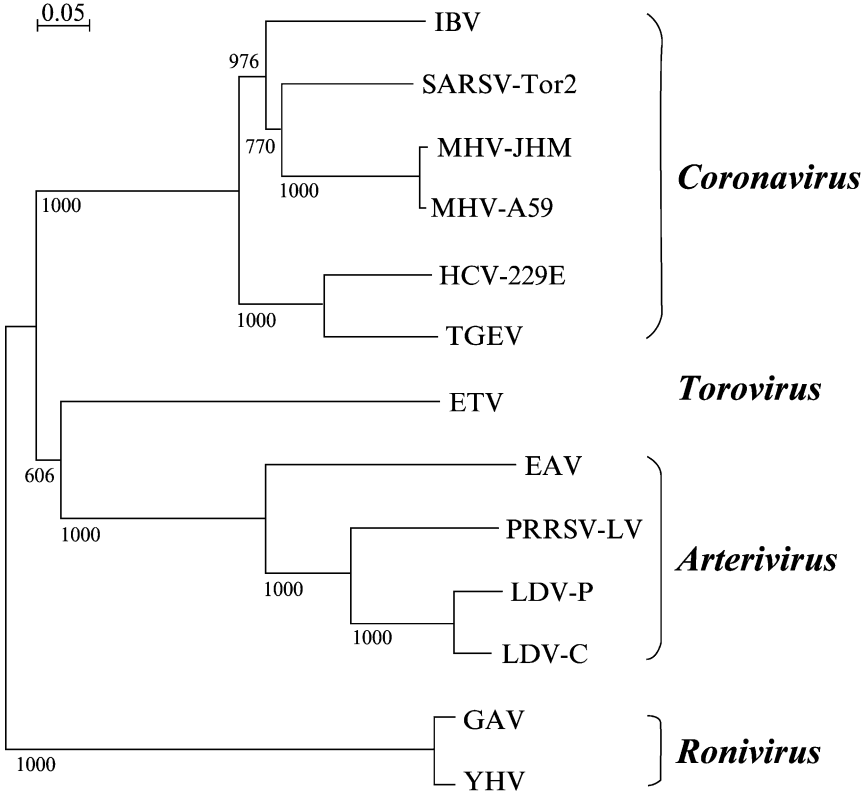

FIG 16. Phylogenetic tree generated using the Clustal X1.81 program employing the Gonnet protein weight matrix for pairwise and multiple alignments and the YHV ORF1b polymerase (RdRp) domain (AAL14793) encompassing residues ^{625}IPKIS$\cdots$IERVF^{907}. The YHV RdRp was aligned to the cognate domains in the pp1ab replicase polyproteins of the *Ronivirus* GAV (AAF82690) as well as species of *Coronavirus* including avian infectious bronchitis virus (IBV, NP_006134), SARSV strain Tor2 (AAP41036), murine hepatitis virus (MHV) strains JHM (VFIHJH) and A59 (CAA36202), human *Coronavirus* strain (HCV strain 229E, Q05002), and porcine transmissible gastroenteritis virus (TGEV strain Purdue, Q91W06). In addition, the alignment was extended to the Berne equine *Torovirus* (ETV, P18458) as well as species of *Arterivirus* including equine arteritis virus (EAV, NP_705590), the porcine reproductive and respiratory syndrome Lelystad virus (PRRSV-LV, Q04561), and the lactate dehydrogenase-elevating virus (LDV) strains P (AAA85664) and C (NP_065671). Bootstrap values are for 1000 independent alignments.

and generated by post-translational processing from a precursor polyprotein (Jitrapakdee *et al.*, 2003). The N terminus of gp116 is generated by cleavage immediately downstream of transmembrane domain 3 motif Ala-Phe-Ala^{228}, and the N terminus of gp64 is

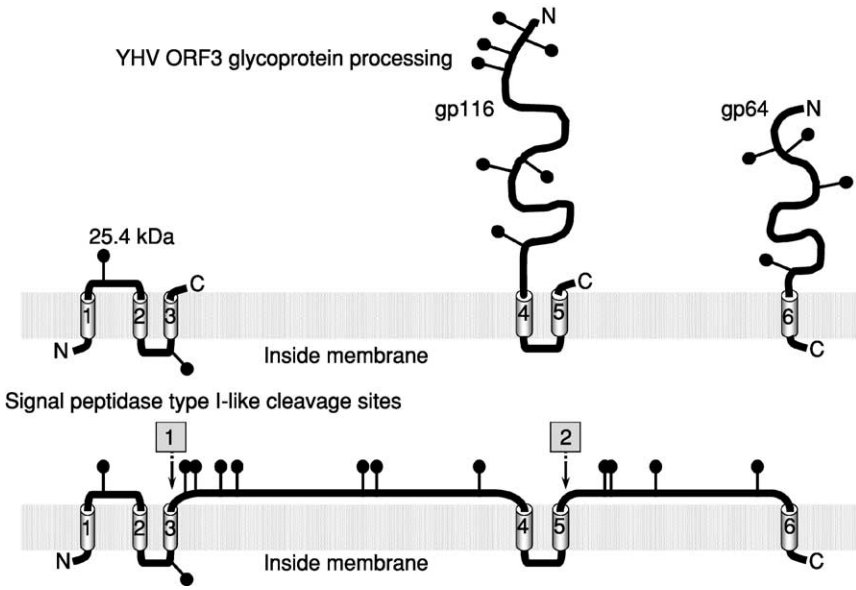

FIG 17. Predicted membrane topology of the YHV ORF3 glycoprotein showing the relative positions of 6 predicted transmembrane (TM) domains and 13 predicted N-linked glycosylation sites. Signal peptidase type I-like cleavage sites that map to residues at the C-terminal side of TM domains 3 and 5 are indicated. The topology of the putative 25.4-kDa triple membrane spanning protein and the gp116 and gp64 structural glycoproteins of YHV generated by cleavage is indicated.

generated by cleavage immediately after the transmembrane domain 5 motif Ala-Ser-Ala^{1127}. Such Ala-X-Ala motifs commonly occur in preprotein signal sequences where they act as a cleavage target for signal peptidase 1 (Carlos *et al.*, 2000), suggesting that ORF3 transmembrane domains 3 and 5 may function as efficient internal signal sequences for a type I-like signal peptidase. The fate of the predicted amino-terminal 25.4-kDa product of the ORF3 polyprotein generated by cleavage at Ala^{228} is not known. No protein of this mass has been detected in purified YHV virions (Jitrapakdee *et al.*, 2003; Nadala *et al.*, 1997b; Wang and Chang, 2000), and specific antibodies are not yet available to detect its expression in infected cells. Although this putative 25.4 kDa protein's function is unknown, it contains three putative membrane spanning domains just as do the nonglycosylated membrane (M) glycoproteins of coronaviruses (Cavanagh, 1995), toroviruses (den Boon *et al.*, 1991), and arteriviruses (Snijder and Meulenberg, 1998). However, its predicted membrane topology infers

an $N_{cyt}C_{exo}$ orientation, which is the reverse of that predicted for the M proteins of vertebrate nidoviruses.

Based on the predicted membrane topology of ORF3, it is probable that (i) gp116 is a polytopic type III transmembrane glycoprotein anchored in the virion envelope by transmembrane domains 4 and 5 with the carboxy-terminus protruding outward and that (ii) gp64 is a type I transmembrane glycoprotein anchored by the C-terminal transmembrane domain 6 of ORF3 (Jitrapakdee *et al.*, 2003). Although gp116 (26 Cys) and gp64 (24 Cys) contain numerous cysteine residues, there is no evidence of intermolecular covalent linkage of these glycoproteins in virions. The lower calculated mass of gp116 (101.7 kDa) and gp64 (58.6 kDa) deduced from the ORF3 sequence is consistent with these proteins being extensively glycosylated at most potential N-linked sites in gp116 (7 sites) and gp64 (4 sites) (Jitrapakdee *et al.*, 2003). Additional analyses, however, are required to determine which of these are used and if any of several predicted O-linked glycosylation sites in gp116 are used.

The 638-nt sequence between ORF3 and the 3′-poly (A) tail of GAV contains a short ORF4 (83 aa = 9.6 kDa) commencing 256 nt downstream of ORF3 (Cowley and Walker, 2002). In YHV, an ORF4 homologue resides 298 nt downstream of ORF3 but only extends 20 amino acids due to a U insertion generating a UAA stop codon (Sittidilokratna, 2003). Because no sgmRNA for ORF4 has been detected in Northern blots, it is unlikely that an ORF4 protein is translated in abundance. However, evidence of ORF4 expression in shrimp tissues at very low levels has been obtained by immuno-histochemistry using antiserum to a GAV ORF4 synthetic peptide (Cowley *et al.*, unpublished data).

In GAV, the intergenic regions (IGRs) upstream of ORF2 (93 nt) and ORF3 (57 nt) contain a highly conserved sequence of 32 nt in which there is a continuous stretch of 26 identical nucleotides (Cowley *et al.*, 2002a). The putative 256-nt intergenic region upstream of ORF4 contains sequences with very limited homology to the two upstream IGRs. In YHV, the IGR upstream of ORF2 is 260 nt longer than in GAV (Sittidilokratna *et al.*, 2002), and sequences flanking a 46-nt (84.8% identity) core sequence conserved in GAV are dissimilar. The 54-nt IGR upstream of YHV ORF3 contains a continuous stretch of 40 nt identical to GAV (Sittidilokratna, 2003). As in GAV, the putative 297-nt IGR upstream of the equivalent ORF4 start site in YHV contains AU-rich sequences, and 40/41 nt in the region immediately upstream of ORF4 are identical (Sittidilokratna, 2003). An alignment of the YHV and GAV IGR sequences encompassing the 5′-terminal position of sgmRNA2 and sgmRNA3 determined for GAV, in addition to a site in

the IGR upstream of ORF4 with limited homology to the conserved promoter elements in the two upstream IGRs, is shown in Fig. 18.

Northern blots in combination with primer extension and 5′-RACE analyses identified two GAV sgmRNAs with 5′-AC termini, in common with the 5′-AC termini of the genomic RNA (Cowley *et al.*, 2000b), that mapped to common 5′-AC sites central to the conserved IGR sequences (Cowley *et al.*, 2002a). This was supported by the identification of intracellular dsRNA replicative intermediates of about 22, 5.8 and 5.2 kbp that approximate the size of genomic RNA1, sgmRNA2, and sgmRNA3, respectively (Cowley *et al.*, 2002a). More recently, a 5′-RACE technique dependent on the presence of 7-methyl-guanosine triphosphate-(^{m7}Gppp)-cap has confirmed the 5′-AC termini of the GAV genomic and sgmRNAs and shown them to be capped (Cowley, unpublished data). The absence of the 5′-leader derived from the 5′-end of the genomic RNA distinguishes GAV from coronaviruses (Sawicki and Sawicki, 1999), arteriviruses (van Marle *et al.*, 1999), and, to a lesser extent, the Berne torovirus (van Vliet *et al.*, 2002). In the latter, only the longest of its four sgmRNAs contains a 5′-leader sequence. No discrete or abundant sgmRNA has been found to initiate in the untranslated sequence upstream of ORF4, which likely explains why it is not translated in abundance. As already described, the genomic IGR sequences encompassing the presumed sgmRNA2 and three transcription start sites are highly conserved between YHV and GAV. It is also noteworthy that, in alignments with the two other IGRs, the single nucleotide variation (U in YHV and G in GAV) in the 41-nt stretch upstream ORF4 occurs at the cognate position of the A residue deduced to be the 5′-terminal nucleotide in sgmRNA2 and sgmRNA3 (Cowley *et al.*, 2002b; Sittidilokratna, 2003). The 5′-AC termini of the genomic RNA and the two sgmRNAs of GAV, and likely YHV, suggest

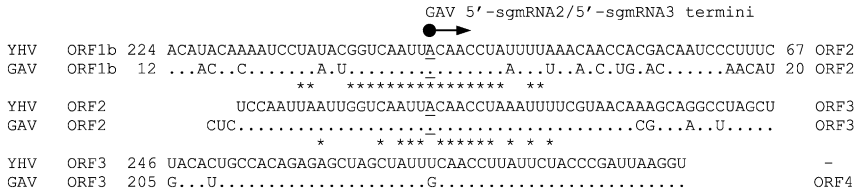

FIG 18. Alignment of the YHV and GAV IGR sequences between the ORF1b–ORF2, ORF2–ORF3, and ORF3–ORF4 genes. Only nucleotide variations in GAV compared to YHV are shown. Conserved nucleotides between the different intergenic sequences are indicated (*), and numbers to the right and left of the sequences indicate the distance to upstream and downstream ORFs. The 5′A terminal positions, determined for GAV and predicted for YHV, sgmRNA2, and sgmRNA3 are underlined.

that the absence of an A nucleotide at this position may critically affect the synthesis of a sgmRNA4 for the efficient translation of ORF4. Therefore, if the expression of ORF4 is not essential to virus replication in its crustacean hosts, mutations interrupting its open reading frame, as detected in YHV (Sittidilokratna, 2003), could accumulate without detriment to virus fitness.

D. Relationship of Yellowhead Virus with Gill-Associated Virus

A bleached appearance of the body and yellowing of the cephalothorax is only sometimes apparent in farmed *P. monodon* with acute YHD and generalized reddening of common in experimental infections (Chantanachookin *et al*., 1993). In original farm outbreaks of acute GAV-related disease, cephalothorax yellowing was not apparent and shrimp typically displayed generalized reddening of the body and gills, which can be reproduced experimentally (Spann *et al*., 1997). YHV appears to be more virulent than GAV in that mortalities can reach 100% within 3 to 4 days in farmed stocks or during experimental infections (Chantanachookin *et al*., 1993; Limsuwan, 1991). However, for GAV, mortalities commonly occur in experimentally infected *P. monodon* over 7 to 14 days, and farm outbreaks often present as a chronic disease involving the progressive appearance of relatively low numbers of moribund shrimp. These infected shrimp usually display shell and gill fouling as well as damaged and melanized appendages, and they gather at the pond edges (Callinan *et al*., 2003b; Owens, 1997; Spann *et al*., 1997; Spann *et al*. unpublished data). No direct comparisons of the pathogenicity of these two related viruses, however, have been reported. Furthermore, meaningful comparisons between YHV and GAV are difficult because inoculum doses have not been standardized in quantal assays, and, in some cases, inocula may have been contaminated with other pathogens.

Although the tissue distribution and histopathology seen in YHV and GAV infections are similar, available reports suggest that there are some differences. High levels of free mature YHV virions accumulate in hemolymph (Nadala *et al*., 1997b; Wongteersupaya *et al*., 1995), whereas it has proved difficult to purify GAV from hemolymph (Spann *et al*., unpublished data). Moreover, intensely basophilic inclusions characteristically seen in the lymphoid organ and elsewhere in YHV-infected shrimp are not as evident for GAV (Spann *et al*., 1997). Although GAV has been identified in the eye of *P. monodon* (Smith, 2000) where it appears to cause lesions reported as retinopathy (Callinan

et al., 2003a), as of yet there are no reports of similar pathology caused by YHV.

Accumulated data now indicate that the reference isolates of YHV from Thailand and GAV from Australia represent two of five distinct genotypes (Cowley *et al.*, 1999; Phan, 2001; Soowannayan *et al.*, 2003; Walker *et al.*, 2001; Wijegoonawardane and Walker, unpublished data) in what has been described as a yellowhead (YH)-complex of viruses (Walker *et al.*, 2001). One of the genotypic variants, with 92% identity to GAV and 83% identity to the reference YHV genotype in the ORF1b gene helicase C-terminal domain, has been found in healthy *P. monodon* broodstock and postlarvae from hatcheries in Vietnam (Phan, 2001; Walker *et al.*, 2001). A variant with 92% identity to GAV and 80% identity to YHV in another ORF1b gene region has been detected in healthy *P. monodon* broodstock from Thailand (Soowannayan *et al.*, 2003). Based on the identity levels to the YHV and GAV reference isolates, it is likely these viruses fall within the same genotype. Sequence comparison of the 577-nt ORF1b region spanned by the GAV5/6 PCR primers originally identified 85% identity between GAV from Australia and a YHV isolate from Thailand (Cowley *et al.*, 1999, 2000a). This GAV region displays similar (83%) identity to the YHV ORF1b sequence determined by Sittidilokratna *et al.* (2002) using a reference Thai YHV isolate derived from diseased shrimp. However, the YHV sequence reported by Cowley *et al.* (1999) is only 85% identical to that reported by Sittidilokratna *et al.* (2002), indicating that it represents a fourth genotype as distantly related to the reference Thai YHV isolate as it is to GAV. Moreover, sequence differences between this variant and the reference YHV genotype might explain why RT-PCR using the GAV5/6 primers generated an amplicon with this YHV genotype (Cowley *et al.*, 2000a) but failed to amplify the reference YHV genotype (Cowley *et al.*, unpublished data). Molecular epidemiological studies have recently identified a fifth YHV genotype in healthy *P. monodon* broodstock from India (Wijegoonawardane and Walker, unpublished data) that is almost equally divergent from GAV (81% identity) and the other three YHV genotypes (80–83% identity) currently recognized within the YH complex of viruses.

E. Diagnosis of Yellowhead Virus

1. Histopathology

The viruses that compose the YH complex (YHV and GAV) produce necrotic lesions in multiple tissues that permit a presumptive diagnosis of this disease by routine H&E histology (Boonyaratpalin *et al.*,

1993; Chantanachookin *et al*., 1993; Lightner, 1996a; Nash *et al*., 1995; OIE, 2003; Spann *et al*., 1997). Both naturally occurring and experimentally induced YHV infections have been reported in a variety of penaeids including *P. monodon, P. japonicus, P. vannamei, P. setiferus, P. aztecus*, and *P. duorarum* (Chantanachookin *et al*., 1993; Lightner, 1996a; Lightner *et al*., 1998; Lu *et al*., 1994; OIE, 2003). The target tissues of YHV are of mesodermal and ectodermal origins and include the LO, hemocytes, fixed phagocytes (heart, gill, and hepatopancreas), hematopoietic tissue, cuticular epithelium, and spongy connective tissues (Fig. 19). Affected cells typically display severe necrosis characterized by nuclear pyknosis, karyorrhexsis or karyolysis, cytoplasmic eosinophilia, and basophilic cytoplasmic inclusions

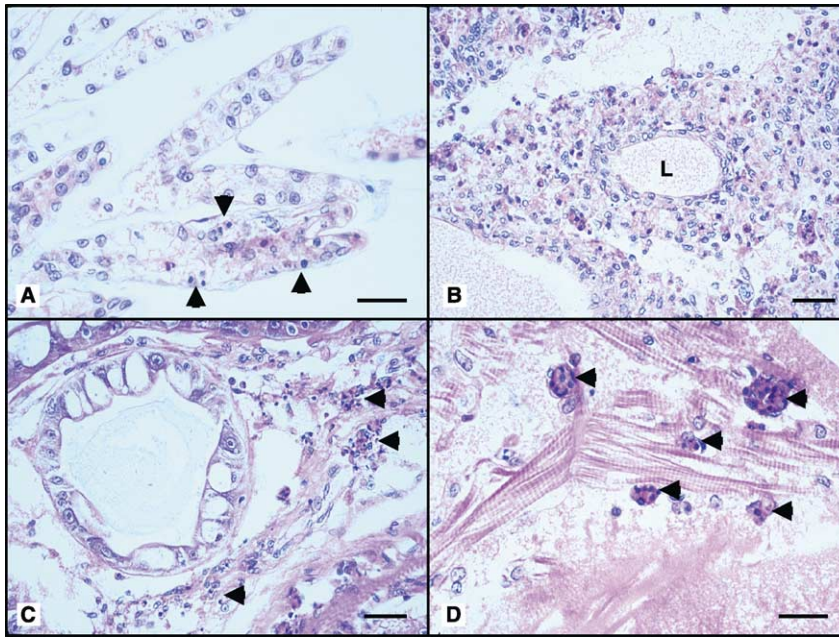

FIG 19. Photomicrographs of tissues from a *Penaeus stylirostris* juvenile with an experimentally induced acute yellowhead virus (Thai strain) infection. (A) Mild YHV-infected gill lamellae displaying multifocal necrotic cells with pyknotic nuclei (arrow heads) and cytoplasmic eosinophilia (B) Severe diffuse necrosis of the stromal matrix cells in the walls of a lymphoid organ arteriole. The numerous basophilic spheres consist of pyknotic nuclei and presumptive inclusion bodies (L = arteriole lumen). (C) Multifocal necrosis (arrow heads) within the intertubular hemal sinuses of the hepatopancreas. (D) Aggregates of necrotic cells, presumably fixed phagocytes (arrow heads), within the heart (Hematoxylin and Eosin stain). Bar: 30 μm.

(Boonyaratpalin *et al.*, 1993; Chantanachookin *et al.*, 1993; Lightner, 1996a; Lu *et al.*, 1994; Nash *et al.*, 1995; OIE, 2003; Spann *et al.*, 1997; Wang and Chang, 2000). These morphological characteristics appear to be caused by apoptosis (Khanobdee *et al.*, 2002) and are very similar to those observed in TSV-infected cuticular epithelial cells. However, the two diseases are easily differentiated as YHV infects a broader range of tissues when compared to TSV (Hasson, 1998; Hasson *et al.*, 1999a,b; Lightner, 1996a). Most notable among the tissues affected by YHV is the LO in which the virus induces a severe diffuse necrosis of the stromal matrix cells in the walls of the LO arterioles (tubules). This pathology is one of the hallmarks of YHD and is not observed in TSV-infected shrimp. The observation of solitary or multiple necrotic fixed phagocytes or hemocytes within the hemal spaces of the heart, hepatopancreas, gills, antennal gland, and connective tissues further aids in histologically differentiating YHV from TSV-caused infections (Boonyaratpalin *et al.*, 1993; Chantanachookin *et al.*, 1993; Lightner, 1996a; Lu *et al.*, 1995a; Nash *et al.*, 1995; OIE, 2003, Spann *et al.*, 1997). Histological lesions that are morphologically similar to those induced by YHV, particularly within the LO, have also been reported for infections caused by WSSV, *Vibrio penaeicida*, and a systemic Rickettsia-like bacterium found in Madagascar (Mermoud *et al.*, 1998; Nunan *et al.*, 2003; Pantoja and Lightner, 2001). Hence, confirmation of a YHV or GAV infection by another diagnostic method (i.e., RT-PCR, ISH, or TEM) is necessary to support presumptive histological findings.

Gill-associated virus is a part of the YHV complex and was described in farmed *P. monodon* from Australia (Spann *et al.*, 1997). By ISH, there is comparable extensive tissue distribution of virus in *P. monodon* acutely infected with either YHV (Tang and Lightner, 1999) or GAV (Spann *et al.*, 2003; Tang *et al.*, 2002). Histologically, GAV differs from YHV in that the lesions are limited to the gills and the lymphoid organ (OIE, 2003; Spann *et al.*, 1997). Similar to TSV, GAV can induce a chronic state infection in *P. monodon* where the only histologic abnormality is the presence of spheroids within the LO (OIE, 2003; Spann *et al.*, 1995; Walker *et al.*, 2003). As in all cases of virus-induced LO spheroids, the causative agent cannot be identified by routine histology, and some other form of diagnostic analysis (i.e., ISH, RT-PCR, or IHC) is required to make this determination.

2. Immunodetection

A nitrocellulose enzyme immunoassay (NC-EIA) using rabbit polyclonal YHV antibody has been described for the detection of YHV (Lu *et al.*, 1996). The gill tissue was a found to be a good source for

the NC-EIA and the detection limit of NC-EIA was 0.4 ng of viral protein. Subsequently, a modified dot-blot NC-EIA using horseradish peroxidase (HRP)-conjugated YHV-specific polyclonal antibody was developed by Nadala and Loh (2000). This assay is very simple and has a potential for screening field samples. A Western blot method capable of detecting YHV in shrimp hemolymph sample has been described by Nadala *et al.* (1997b). Using this method, a 135-kDa protein and a 170-kDa protein of YHV was detected in hemolymph at 64 hr post-infection, and a 135-kDa protein was detected in YHV-infected primary lymphoid organ cell culture 4 days post-infection. The Western blot assay is highly specific and is recommended by the OIE as a confirmatory diagnostic method for YHV detection in combination with *in situ* nucleic acid hybridization, transmission electron microscopy (TEM), and RT-PCR (OIE, 2003). A YHV-specific monoclonal antibody (mAbV3-2B) was used for the detection of the virus by immunohistochemical examination and by Western blot analysis (Sithigorngul *et al.*, 2000). The mAb showed YHV-specific immunoreactivities in the cytoplasm of gill tissues and in hemocytes and detected a 135-kDa protein in Western blots (Sithigorngul *et al.*, 2000).

3. RT-PCR and Real-Time RT-PCR

The first protocol for YHV detection by RT-PCR was described by Wongteerasupaya *et al.* (1997). The primer sequences have been provided in Table II. The RT-PCR amplifies a 135-bp region in the ORF1b gene (Cowley *et al.*, 1999; Sittidilokratna *et al.*, 2002), and the method has a sensitivity of approximately 0.01 pg of YHV RNA ($\sim 10^3$ genomes). Tang and Lightner (1999) also described an RT-PCR method using YHV-specific primers amplifying a 273-bp ORF1b gene region upstream of the 135-bp amplicon; the test detected YHV in the hemolymph of infected shrimp (Table II). An RT-nested PCR has also been described for GAV (Cowley *et al.*, 2000a), and recently, Cowley *et al.* (2004b) have described another nested RT-PCR that is highly sensitive and capable of differentiating YHV from GAV. The latter method involves amplification of a 749-bp ORF1b region of either YHV or GAV in the first step of PCR. In the second step of PCR, either a 406-bp cDNA is amplified from GAV or a 277-bp cDNA is amplified from YHV using GAV- and YHV-specific primers (Fig. 20, Table II). The two-step PCR was found to be about 1000-fold more sensitive than the one-step PCR, and the detection limit was found to be 10 fg of total cellular RNA. Amplification of both the 406-bp and 277-bp products from the same sample allows the identification of dual infections with YHV and GAV (Cowley *et al.*, 2004a).

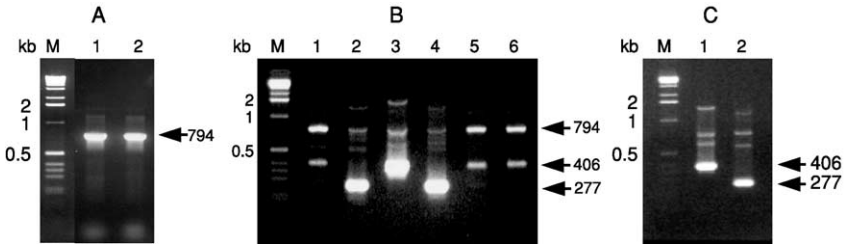

FIG 20. Amplification of GAV and YHV RNA by RT-PCR followed by nested PCR with various primer combinations. (A) PCR amplification (primer pair GY1–GY4) of a 794-bp product from cDNA synthesized from reference GAV (lane 1) and YHV (lane 2) RNA using primer GY5. (B) Nested PCR amplification of RT-PCR products from GAV (lanes 1–3) and YHV (lanes 4–6) using primer pairs GY2–Y3 (lanes 1 and 4), GY2–G3 (lanes 2 and 5), and GY2–G6 (lanes 3 and 6). (C) Nested PCR amplification of a 406-bp GAV-specific product (lane 1) or 277-bp YHV-specific product (lane 2) using the multiplexed primer set GY2–Y3/G6. PCR products (10 μl) were resolved in a 2% agarose-TAE gel containing 0.5 μg/ml ethidium bromide. M: 1-kb DNA ladder (Invitrogen). Reproduced from Cowley *et al.* (2004a), with permission.

Real-time RT-PCR methods for the detection and quantification of YHV RNA using SYBR Green chemistry have recently been described (Dhar *et al.*, 2002; Mouillesseaux *et al.*, 2003). The methods vary in the length of the amplicon (50 to 98 bp) generated using YHV-specific primers (Table II). The method is capable of detecting down to a single-copy equivalent of the YHV genome and has a wide dynamic range of detection. The amplification plots and the corresponding dissociation curves of a YHV amplicon and a shrimp internal control gene are shown in Fig. 21. The specificity of the YHV amplicon is confirmed by examining the dissociation curves. A dissociation curve with a single peak at expected melting temperature indicates the amplification target amplicon. Because each amplicon has a unique melting temperature, primers based on a conserved region in the genome will be useful to amplify all the genotypes of YHV/GAV complex, whereas primers based on the variable region of the genome will be useful in identifying different genotypes of YHV–GAV complex. In addition, due to the lack of an immortalized shrimp cell line, quantification of the virus is difficult. Although YHV has been cultivated in a primary cell line from the lymphoid organ of *P. vannamei* (Lu *et al.*, 1995b) or *P. monodon* (Chen and Wang, 1999), the need to prepare cultures from shrimp with an unknown background presents a problem for standardization of the virus assay. This limitation can be overcome by real-time RT-PCR. In addition, real-time RT-PCR could be used to detect subclinical infection, measure the viral load, and determine the tissue tropism for YHV

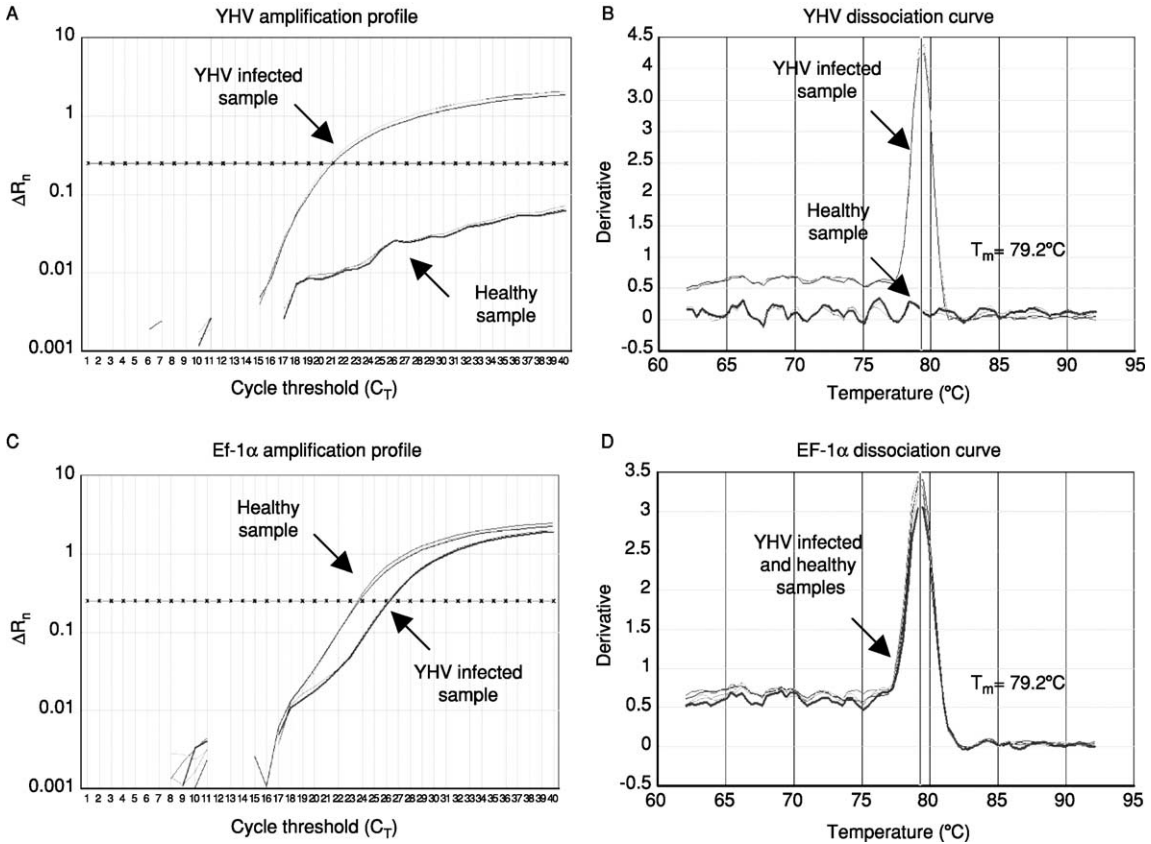

FIG. 21. The amplification plots and the corresponding dissociation curves of YHV and EF-1α genes from a TSV infected shrimp and a healthy shrimp. The melting temperature (Tm) of each amplicon is shown alongside its dissociation curve. Adapted from Dhar *et al*. (2002) with permission.

and GAV. Although real-time RT-PCR may not be feasible for routine field testing due to high cost, sophisticated instrumentation, and the required technical expertise, it would be useful for testing broodstock to ensure their virus-free status and monitoring of live and frozen shrimp that are sold within and between countries with the objective of preventing the further spread of these viruses.

IV. Concluding Remarks

Taura syndrome and yellowhead diseases have had a profound economic and social impact in the developing nations of East Asia and the Americas where they have threatened the long-term sustainability of numerous shrimp culture industries. A variety of management strategies, including virus exclusion or prevention through the use of specific pathogen-free (SPF) and/or specific pathogen-resistant (SPR) stocks, have been attempted (Lightner, 1999). However, the ability of RNA viruses, such as TSV and YHV, to mutate and adapt to previously resistant hosts makes their control and exclusion particularly difficult. Advances in the areas of TSV and YHV detection have facilitated the development of highly sensitive and disease-specific molecular diagnostic tools that permit the nonlethal detection of subclinically infected shrimp populations. This enables farmers to identify and eliminate contaminated stocks and, thus, limit the spread of these viral diseases.

There has been significant progress in understanding the general biology of both TS and YHD and in developing methods for the detection of TSV and YHV. However, many of the processes involved in viral replication and translation of the viral encoded genes remain to be determined. The molecular mechanisms used for the initiation and regulation of viral RNA synthesis and the regulation of translation and processing of the nonstructural and structural polyproteins encoded by the TSV and YHV will be the subjects of future studies. Studying these processes will be critical toward understanding the molecular basis of TSV and YHV pathogenesis.

Another area that has received very little attention is the pathogen defense or immune response of shrimp against viral diseases. Information pertaining to shrimp genes that might be involved in the pathogenesis of TSV and YHV and viral diseases in general remains elusive. Most studies on the immunity of shrimp and crustaceans have focused in general on bacterial and fungal pathogens, and little is known about how crustaceans respond to viral infections. Although no host cellular genes involved in TSV and YHV pathogenesis have been identified so

far, a number of immune genes in shrimp that might be involved in WSSV pathogenesis have been identified by using mRNA differential display (Astrofsky *et al.*, 2002; Luo *et al.*, 2003), expressed sequence tag analysis (Rojtinnakorn *et al.*, 2002; Roux *et al.*, 2002,), and cDNA microarray analysis (Dhar *et al.*, 2003). Functional genomics approaches, using shrimp cDNA microarrays coupled with targeted gene silencing by dsRNA interference, should prove useful in identifying the genes and the molecular events governing viral pathogenesis in TSV and YHV.

Acknowledgments

Arun K. Dhar would like to thank Refugio Robles-Sikisaka and Kate Licon for their help in preparing the manuscript. Research work of Dhar is funded by grants from Advanced Bionutrition Corporation, Columbia, Maryland, and the California Sea Grant Program, California. Kenneth W. Hasson would like to thank Dr. Patricia Varner, Mr. Daniel Areola, and Dr. John Reagor of TVMDL for their editorial comments on portions of the manuscript and image scanning assistance.

References

Albaladejo, J. D., Tapay, L. M., Migo, V. P., Alfafara, C. G., Somga, J. R., Mayo, S. L., Miranda, R. C., Natividad, K., Magbanua, F. O., Itami, T., Matsumura, M., Nadala, E. C. B., Jr., and Loh, P. C. (1998). Screening for shrimp viruses in the Philippines. *In* "Advances in Shrimp Biotechnology" (T. W. Flegel, ed.). National Center for Genetic Engineering and Biotechnology, Bangkok, Thailand.

Anggraeni, M. S., and Owens, L. (2000). The haemocytic origin of lymphoid organ spheroid cells in the penaeid prawn *Penaeus* monodon. *Dis. Aqua. Org.* **40:**85–92.

Anonymous (1995). Mortalidades en Texas no es sindrome de Taura. Panorama Acuicola **1:**1 and 6.

Argue, B. J., Arce, S. M., Lotz, J. M., and Moss, S. M. (2002). Selective breeding of pacific white shrimp (*Litopenaeus vannamei*) for growth and resistance to Taura syndrome virus. *Aquaculture* **204:**447–460.

Astrofsky, A., Roux, M. M., Klimpel, K. R., Fox, J. G., and Dhar, A. K. (2002). Identification of differentially expressed genes in Pacific blue shrimp (*Penaeus stylirostris*) in response to challenge with white spot virus (WSSV). *Arch. Virol.* **147:**1799–1812.

Barniol, R. (1995). Etiologia del sindrome de Taura: La tesis Ecuatoriana. *Acuacultura del Ecuador* **10:**7–11.

Bell, T. A., and Lightner, D. V. (1988). "A Handbook of Normal Penaeid Shrimp Histology." World Aquaculture Society, Baton Rouge, LA.

Bonami, J. R., Hasson, K. W., Mari, J., Poulos, B. T., and Lightner, D. V. (1997). Taura syndrome of marine penaeid shrimp: Characterization of the viral agent. *J. Gen. Virol.* **78:**313–319.

Boonyaratpalin, S., Supamataya, K., Kasornchnadra, J., Direkbusarakom, S., Aekpanithanpong, U., and Chantanachookin, C. (1993). Non-occluded baculo-like virus, the causative agent of yellow-head disease in the black tiger shrimp (*Penaeus monodon*). *Fish Pathol.* **28:**103–109.

Brock, J. A. (1997). Special topic review: Taura syndrome, a disease important to shrimp farms in the Americas. *World J. Microbiol. Biotechnol.* **13:**415–418.

Brock, J. A., Gose, R., Lightner, D. V., and Hasson, K. W. (1995). An overview on Taura syndrome, an important disease of farmed *Penaeus vannamei*. *In* "Swimming Through Troubled Water" (C. L. Browdy and J. S. Hopkins, eds.). *Proceedings of the Special Session on Shrimp Farming Aquaculture*,World Aquaculture Society, Baton Rouge, LA.

Brock, J. A., Gose, R. B., Lightner, D. V., and Hasson, K. W. (1997). Recent developments and an overview of Taura syndrome of farmed shrimp in the Americas. *In* "Diseases in Asian Aquaculture III" (T. W. Flegel and I. H. MacRae, eds.). Fish Health Section Asian Fisheries Society, Manila, Philippines.

Callinan, R. B., Jiang, L., Smith, P. T., and Soowannayan, C. (2003a). Fatal, virus-associated peripheral neuropathy and retinopathy in farmed *Penaeus monodon* in eastern Australia. *Dis. Aquat. Org.* **53:**181–193.

Callinan, R. B., and Jiang, L. (2003b). Fatal, virus-associated peripheral neuropathy and retinopathy in farmed *Penaeus monodon* in eastern Australia. *Dis. Aquat. Org.* **53:**195–202.

Carlos, J. L., Paetzel, M., Brubaker, G., Karla, A., Ashwell, C. M., Lively, M. O., Cao, G., Bullinger, P., and Dalbey, R. E. (2000). The role of the membrane-spanning domain of type I signal peptidases in substrate cleavage site selection. *Biol. Chem.* **275:**38813–38822.

Carr, W. H., Fjalestad, K. T., Lotz, J. M., Oyama, R. N., Godin, D. M., Chang, C. P. L., Segura, F. J., Roddy, S. C., and Sweeney, J. N. (1997). Advances in selective breeding for growth performance and disease resistance in specific pathogen-free (SPF) pacific white shrimp, *Penaeus vannamei*. *Linking Science to Sustainable Industry Development, Annual International Conference and Exposition of the World Aquaculture Society* **Vol 52:**68.

Cavanagh, D. (1995). The coronavirus surface glycoprotein. *In* "The Coronaviridae" (S. G. Siddell, ed.). Plenum Press, New York.

Chantanachookin, C. S., Boonyaratpalin, J., Kasornchnadra, S., Direkbusarakom, U., Ekpanithanpong, K., Supamataya, S., Sriurairatana, T., and Flegel, W. (1993). Histology and ultrastructure reveal a new granulosis-like virus in *Penaeus monodon* affected by yellowhead disease. *Dis. Aqua. Org.* **17:**145–157.

Chen, S. N., and Kou, G. H. (1989). Infection of cultured cells from the lymphoid organ of *Penaeus monodon* Fabricius by monodon-type baculovirus. *J. Fish Dis.* **12:**73–76.

Chen, S. N., and Wang, C. S. (1999). Establishment of cell culture systems from penaeid shrimp and their susceptibility to white spot disease and yellowhead viruses. *Methods Cell. Sci.* **21:**199–206.

Clifford, H. (2000). Shrimp farming in Mexico: Recent developments. *Glob. Aquaculture Adv.* **3:**79–81.

Christian, P. D., and Scotti, P. D. (1998). Picorna-like viruses of insects. *In* "The Insect Viruses" (L. K. Miller and K. A. Ball, eds.). Plenum Press, New York.

Couch, J. A. (1974a). Free and occluded virus similar to *Baculovirus* in hepatopancreas of pink shrimp. *Nature* **247:**229–231.

Couch, J. A. (1974b). An enzootic nuclear polyhydrosis virus of pink shrimp: Ultrastructure, prevalence, and enhancement. *J. Inv. Pathol.* **24:**311–331.

Cowley, J. A., and Walker, P. J. (2002). The complete genome sequence of gill-associated virus of *Penaeus monodon* prawns indicates a gene organisation unique among nodoviruses. *Arch. Virol.* **147:**1977–1987.

Cowley, J. A., Dimmock, C. M., Wongteerasupaya, C., Boonsaeng, V., Panyim, S., and Walker, P. J. (1999). Yellowhead virus from Thailand and gill-associated virus from

Australia are closely related but distinct prawn viruses. *Dis. Aquat. Org.* **36:**153–157.

Cowley, J. A., Dimmock, C. M., Spann, K. M., and Walker, P. J. (2000a). Detection of Australian gill-associated virus (GAV) and lymphoid organ virus (LOV) of *Penaeus monodon* by RT-nested PCR. *Dis. Aquat. Org.* **39:**159–167.

Cowley, J. A., Dimmock, C. M., Spann, K. M., and Walker, P. J. (2000b). Gill-associated virus of *Penaeus monodon* prawns: An invertebrate virus with ORF1a and ORF1b genes related to arteri- and coronaviruses. *J. Gen. Virol.* **81:**1473–1484.

Cowley, J. A., Dimmock, C. M., Spann, K. M., and Walker, P. J. (2001). Gill-associated virus of *Penaeus monodon* prawns. Molecular evidence for the first invertebrate nidovirus. *Adv. Exp. Med. Biol.* **494:**43–48.

Cowley, J. A., Dimmock, C. M., and Walker, P. J. (2002a). Gill-associated nidovirus of *Penaeus monodon* prawns transcribes 3′-coterminal subgenomic mRNAs that do not possess 5′-leader sequences. *J. Gen. Virol.* **83:**927–935.

Cowley, J. A., Hall, M. R., Cadogan, L. C., Spann, K. M., and Walker, P. J. (2002b). Vertical transmission of gill-associated virus (GAV) in the black tiger prawn *Penaeus monodon*. *Dis. Aquat. Org.* **50:**95–104.

Cowley, J. A., Cadogan, L. C., Wongteerasupaya, C., Hodgson, R. A., J., Boonsaeng, V., Walker, P. J. (2004a). Multiplex RT-nested PCR differentiation of gill-associated virus (Australia) from yellowhead virus (Thailand) of *Penaeus monodon*. *J. Virol. Methods* **17**: 49–59.

Cowley, J. A., Cadogan, L. C., Spann, K. M., Sittidilokratna, N., Walker, P. J. (2004b). The gene encoding the nucleocapsid protein of gill-associated nidovirus of *Penaeus monodon* prawns is located upstream of the glycoprotein gene. *J. Virol.* **78**: 8935–8941.

de Vries, A. A. F., Horzinek, M. C., Rottier, P. J. M., and de Groot, R. J. (1997). The genome organization of the *Nidovirales*: Similarities and differences between arteri-, toro-, and coronaviruses. *Seminars Virol.* **8:**33–47.

den Boon, J. A., Snijder, E. J., Locker, J. K., Horzinek, M. C., and Rottier, P. J. (1991). Another triple-spanning envelope protein among intracellularly budding RNA viruses: The torovirus E protein. *Virology* **182:**655–663.

Dhar, A. K., Roux, M. M., and Klimpel, K. R. (2002). Quantitative assay for measuring the Taura syndrome virus (TSV) and yellowhead virus (YHV) load in shrimp by real-time RT-PCR using SYBR Green chemistry. *J. Virol. Methods* **104:**69–82.

Dhar, A. K., Dettori, A., Roux, M. R., Klimpel, K. R., and Read, B. (2003). Use of cDNA microarray to isolate the differentially expressed genes in white spot syndrome virus (WSSV) infected shrimp (*Penaeus stylirostris*). *Arch. Virol.* **148:**2381–2396.

Domingo, E., and Holland, J. J. (1997). RNA virus mutation and fitness for survival. *Annu. Rev. Microbiol.* **51:**151–178.

Erickson, H., Lawrence, A. L., Gregg, K. L., Frelier, P. F., Lotz, J. M., and McKee, D. A. (1997). Sensitivity of *Penaeus vannamei, Sciaenops ocellatus, Cynoscion nebulosus, Palaemonetes* sp., and *Callinectes sapidus* to Taura syndrome virus infected tissue. *Linking Science to Sustainable Industry Development, Annual International Conference and Exposition of the World Aquaculture Society* **Vol 52:**140.

Erickson, H., Zarain-Herberg, M., and Lightner, D. V. (2002). Detection of Taura syndrome virus (TSV) strain differences using selected diagnostic methods: Diagnostic implications in penaeid shrimp. *Dis. Aqua. Org.* **52:**1–10.

Fitch, W. M., Leiter, J. M., Li, X. O., and Palese, P. (1991). Positive Darwinian evolution in human influenza A viruses. *Proc. Natl. Acad. Sci.* **88:**4270–4274.

Flegel, T. W. (1997). Special topic review: Major viral diseases of the black tiger prawn *(Penaeus monodon)* in Thailand. *World J. Microbiol. Biotechnol.* **13:**433–442.

Flegel, T. W., Fegan, D. F., and Sriurairatana, S. (1995a). Environmental control of infectious shrimp diseases in Thailand. *In* "Diseases in Asian Aquaculture II" (M. Shariff, R. P. Subasinghe, and J. R. Arthur, eds.). Asian Fisheries Society, Manila, Philippines.

Flegel, T. W., Sriurairatana, S., Wongterrasupaya, C., Boonsaeng, V., Panyim, S., and Withyachumnarnkul, B. (1995b). Progress in characterization and control of yellow-head virus of *Penaeus monodon*. *In "Swimming Through Troubled Water"* (C. L. Braudy and J. S. Hopkins, eds.). Proceedings of the Special Session on Shrimp Farming Aquaculture, World Aquaculture Society, Baton Rouge, LA.

Flegel, T. W., Boonyaratpalin, S., and Withyachumnarnkul, B. (1997a). Current status of research on yellowhead virus and white spot virus in Thailand. *In* "Diseases in Asian Aquaculture III" (T. W. Flegel and I. H. MacRae, eds.), pp. 285–296. Fish Health Section. Asian Fisheries Society, Manila, Philippines.

Flegel, T. W., Sriurairatana, S., Morrison, D. J., and Waiyakrutha, N. (1997b). *Penaeus monodon* captured broodstock surveyed for yellowhead virus and other pathogens by electron microscopy. *In* "Shrimp Biotechnology in Thailand" (T. W. Flegel, P. Menasveta, and S. Paisarnrat, eds.), National Center for Genetic Engineering and Biotechnology, Bangkok, Thailand, pp. 37–43.

Garza, J. R., Hasson, K. W., Poulos, B. T., Redman, R. M., White, B. L., and Lightner, D. V. (1997). Demonstration of infectious Taura syndrome virus in the feces of sea gulls collected during an epizootic in Texas. *J. Aquat. Animal Health* **9:**156–159.

González, J. M., Gomez-Puertas, P., Cavanagh, D., Gorbalenya, A. E., and Enjuanes, L. (2003). A comparative sequence analysis to revise the current taxonomy of the family Coronaviridae. *Arch. Virol.* **148:**2207–2235.

Gorbalenya, A. E., and Koonin, E. V. (1989). Viral proteins containing the purine NTP-binding sequence pattern. *Nucl. Acids. Res.* **17:**4847–4861.

Gorbalenya, A. E., Blinov, V. M., Donchenko, A. P., and Koonin, E. V. (1989). An NTP-binding motif is the most conserved sequence in a highly diverged monophyletic group of proteins involved in positive strand RNA viral replication. *J. Mol. Evol.* **28:**256–268.

Gorbalenya, A. E., Pringle, F. M., Zeddam, J. L., Luke, B. T., Cameron, C. E., Kalmakoff, J., Hanzlik, T. N., Gordon, K. H., and Ward, V. K. (2002). The palm subdomain-based active site is internally permuted in viral RNA-dependent RNA polymerases of an ancient lineage. *J. Mol. Biol.* **324:**47–62.

Halim, S., and Ramsingh, A. I. (2000). A point mutation in VP1 of coxsackie virus B4 alters antigenicity. *Virology* **269:**86–94.

Hasson, K. W., Lightner, D. V., Poulos, B. T., Redman, R. M., White, B. L., Brock, J. A., and Bonami, J. R. (1995). Taura Syndrome in *Penaeus vannamei*: Demonstration of a viral etiology. *Dis. Aqua. Org.* **23:**115–126.

Hasson, K. W., Hasson, J., Aubert, H., Redman, R. M., and Lightner, D. V. (1997). A new RNA-friendly fixative for the preservation of penaeid shrimp samples for virological detection using cDNA genomic probes. *J. Virol. Methods* **66:**227–236.

Hasson, K. W. (1998). Taura Syndrome in Marine Penaeid Shrimp: Discovery of the Viral Agent and Disease Characterization Studies. Ph.D. diss. University of Arizona, Tucson.

Hasson, K. W., Lightner, D. V., Mohney, L. L., Redman, R. M., Poulos, B. T., Mari, J., Bonami, J. R., and Brock, J. A. (1999a). The geographic distribution of Taura syndrome virus (TSV) in the Americas: Determination by histopathology and *in situ* hybridization using TSV-specific cDNA probes. *Aquaculture* **171:**13–26.

Hasson, K. W., Lightner, D. V., Mohney, L. L., Redman, R. M., Poulos, B. T., and White, B. L. (1999b). Taura syndrome virus (TSV) lesion development and the disease cycle in the Pacific white shrimp *Penaeus vannamei*. *Dis. Aqua. Org.* **36:**81–93.

Hasson, K. W., Lightner, D. V., Mohney, L. L., Redman, R. M., Poulos, B. T., and White, B. L. (1999c). Role of lymphoid organ spheroids in chronic Taura syndrome virus (TSV) infections in *Penaeus vannamei*. *Dis. Aqua. Org.* **38:**93–105.

Haydon, D. T., Bastos, A. D., Knowles, N. J., and Samuel, A. R. (2001). Evidence for positive selection in foot-and-mouth disease virus capsid genes from field isolates. *Genetics* **157:**7–15.

Holland, P. M., Abramson, R. D., Watson, R., and Gelfard, G. H. (1991). Detection of specific polymerase chain reaction product by utilizing the 5′–3′ exonuclease activity of *Thermas aquaticus* activity. *Proc. Natl. Acad. Sci. USA* **88:**7276–7280.

Humason, G. L. (1972). "Animal Tissue Techniques," 3rd Ed. W. H. Freeman and Company, San Francisco.

Intriago, P., Espinoza, J., Jimenez, R., Machuca, M., Barniol, R., Krauss, E., and Salvador, X. (1995a). Taura syndrome, a toxicity syndrome of *Penaeus vannamei* in Ecuador. *Annual International Conference and Exposition of the World Aquaculture Society,* p. 143.

Intriago, P., Jimenez, R., Machuca, M., Barniol, R., Krauss, E., and Salvador, X. (1995b). Demonstracion de la etiologia toxica del sindrome de Taura. *Tercero Congresso Ecuatoriano de Acuicultura,* p. 23.

Intriago, P., Jimenez, R., Machuca, M., Barniol, R., Krauss, E., and Salvador, X. (1997a). Evidencias bioquimicas y experimentales que apoyan la naturaleza toxica del sindrome de Taura en *Penaeus vannamei* (*Crustacea decapoda*) en el Ecuador. *Panorama Acuicola* **2:**22–23.

Intriago, P., Jimenez, R., Machuca, M., Barniol, R., Krauss, E., and Salvador, X. (1997b). Experiments on toxicosis as the cause of Taura syndrome in *Penaeus vannamei* (*Crustacea decapoda*) in Ecuador. *In* "Diseases in Asian Aquaculture III" (T. W. Flegel and I. H. MacRae, eds.). Fish Health Section, Asian Fisheries Society, Manila, Philippines.

Jimenez, R. (1992). Sindrome de taura (Resumen). *Acua. Ecuador* **1:**1–16.

Jimenez, R., Machuca, M., and Barniol, L. (1995). Taura syndrome: Epizootiology and histopathology of a mortality toxicity syndrome of penaeid shrimp in Ecuador. *Annual International Conference and Exposition of the World Aquaculture Society,* p. 147.

Jimenez, R., Barniol, R., Barniol, L., and Machuca, M. (2000). Periodic occurrence of epithelial viral necrosis outbreaks in *Penaeus vannamei* in Ecuador. *Dis. Aqua. Org.* **42:**91–99.

Jitrapakdee, S., Unajak, S., Sittidilokratna, N., Hodgson, R. A. J., Cowley, J. A., Walker, P. J., Panyim, S., and Boonsaeng, V. (2003). Identification and analysis of gp116 and gp64 structural glycoproteins of yellowhead nidovirus of *Penaeus monodon* shrimp. *J. Gen. Virol.* **84:**863–873.

Jory, D. (1995). Global situation and current megatrends in marine shrimp farming. *Aquaculture* **21:**74–83.

Khanobdee, K., Soowannayan, C., Flegel, T. W., Ubol, S., and Withyachumnarnkul, B. (2002). Evidence for apoptotic correlated with mortality in the giant black tiger shrimp *Penaeus monodon* infected with yellowhead virus. *Dis. Aquat. Org.* **48:**79–90.

Khoa, L. V., Hao, N. V., and Huong, L. T. L. (2000). Vietnam. *In* "Thematic Review on Management Strategies for Major Diseases in Shrimp Aquaculture" (J. R. Arthur, D. Fegan, and R. Subasinghe, eds.). FAO, Rome, Italy.

Koonin, E. V. (1991). The phylogeny of RNA-dependent RNA polymerases of positive-strand RNA viruses. *J. Gen. Virol.* **72:**2197–2206.

Kondo, M., Itami, T., Takahashi, Y., Fuji, R., and Tomonga, S. (1994). Structure and function of the lymphoid organ in the Kuruma prawn. *Dev. Comp. Immunol.* **18**(Suppl. 1):109.

Kozak, M. (1986). Point mutations define a sequence flanking the AUG initiator codon that modulates translation by eukaryotic ribosomes. *Cell* **44:**283–292.

Lightner, D. V. (1995). Taura syndrome: An economically important viral disease impacting the shrimp farming industries of the Americas including the United States. *Proceedings of the Ninety-Ninth Annual Meeting USAHA,* pp. 36–62.

Lightner, D. V. (1996a). A Handbook of Shrimp Pathology and Diagnostic Procedures for Diseases of Cultured Penaeid Shrimp. World Aquaculture Society, Baton Rouge, LA.

Lightner, D. V. (1996b). Epizootiology, distribution, and the impact on international trade of two penaeid shrimp viruses in the Americas. *Rev. Sci. Off. Int. Epiz.* **5:**579–601.

Lightner, D. V. (1999). The penaeid shrimp viruses TSV, IHHNV, WSSV, and YHV: Current status in the Americas, available diagnostic methods, and management strategies. *J. Appl. Aquaculture* **9:**27–51.

Lightner, D. V., and Redman, R. M. (1998). Shrimp diseases and current diagnostic methods. *Aquaculture* **164:**201–220.

Lightner, D. V., Jones, L. S., and Ware, G. W. (1994). *Proceedings of the Taura Syndrome Workshop.* Executive summary, submitted reports, and transcribed notes.

Lightner, D. V., Redman, R. M., Hasson, K. W., and Pantoja, C. R. (1995). Taura syndrome in *Penaeus vannamei*: Histopathology and ultrastructure. *Dis. Aqua. Org.* **21:**53–59.

Lightner, D. V., Hasson, K. W., White, B. L., and Redman, R. M. (1996). Chronic toxicological and histopathological studies with benomyl in *Penaeus vannamei* (Crustacea: Decapoda). *Aquat. Toxicol.* **34:**105–118.

Lightner, D. V., Redman, R. M., Poulos, B. T., Nunan, L. M., Mari, J. L., Hasson, K. W., and Bonami, J. R. (1997a). Taura syndrome: Etiology, pathology, hosts, geographic distribution, and detection methods. *New approaches to viral diseases of aquatic animals, Proceedings of the NRIA Workshop,* pp. 190–205.

Lightner, D. V., Redman, R. M., Poulos, B. T., Nunan, L. M., Mari, J. L., and Hasson, K. W. (1997b). Risk of spread of penaeid shrimp viruses in the Americas by the international movement of live and frozen shrimp. *Rev. Sci. Off. int. Epiz.* **16:**146–160.

Lightner, D. V., Hasson, K. W., White, B. L., and Redman, R. M. (1998). Experimental infection of Western Hemisphere penaeid shrimp with Asian white spot syndrome virus and Asian yellowhead virus. *J. Aquat. Anim. Health* **10:**271–281.

Limsuwan, C. (1991). "Handbook for Cultivation of Black Tiger Prawns." Tansetakit, Bangkok, Thailand.

Loh, P. C., Tapay, L. M., Lu, Y., and Nadala, E. C. B., Jr. (1997). Viral pathogens of the penaeid shrimp. *Adv. Virus Res.* **48:**263–312.

Loh, P. C., Cesar, E., Nadala, B., Jr., Tapay, L. M., and Lu, Y. (1998). Recent developments in immunologically based and cell culture protocols for the specific detection of shrimp viral pathogens. *In* "Advances in Shrimp Biotechnology" (T. W. Flegel, ed.). National Center for Genetic Engineering and Biotechnology, Bangkok, Thailand.

Lotz, J. (1997). Effect of host size on virulence of Taura virus to the marine shrimp *Penaeus vannamei* (Crustacea: Penaeidae). *Dis. Aquat. Org.* **30:**45–51.

Lotz, J., Flowers, A. M., and Breland, V. (2003). A model of Taura syndrome virus (TSV) epidemics in *Litopenaeus vannamei*. *J. Invert. Pathology* **83:**168–176.

Lu, Y., Tapay, L. M., Brock, J. A., and Loh, P. C. (1994). Infection of the yellowhead baculo-like virus (YBV) in two species of penaeid shrimp, *Penaeus stylirostris* (Simpson) and *Penaeus vannamei* (Boone). *J. Fish Dis.* **17:**649–656.

Lu, Y., Tapay, L. M., Loh, P. C., Brock, J. A., and Gose, R. B. (1995a). Distribution of yellowhead virus in selected tissues and organs of penaeid shrimp *Penaeus vannamei*. *Dis. Aquat. Org.* **23:**67–70.

Lu, Y., Tapay, L. M., Loh, P. C., Brock, J. A., and Gose, R. B. (1995b). Development of a quantal assay in primary shrimp cell culture for yellowhead baculovirus (YBV) of penaeid shrimp. *J. Virol. Methods* **52:**231–236.

Lu, Y., Tapay, L. M., and Loh, P. C. (1996). Development of a nitrocellulose-enzyme immunoassay (NC-EIA) for the detection of yellowhead virus from penaeid shrimp. *J. Fish Dis.* **19:**9–13.

Lu, Y., Tapay, L. M., Gose, R. B., Brock, J. A., and Loh, P. C. (1997). Infectivity of yellowhead virus (YHV) and the Chinese baculo-like virus (CBV) in two species of penaeid shrimp, *Penaeus stylirostris* (Stimpson) and *Penaeus vannamei* (Boone). *In* "Diseases in Asian Aquaculture III" (T. W. Flegel and I. H. MacRae, eds.). Asian Fisheries Society, Manila, Philippine.

Luo, T., Zhang, X., Shao, Z., and Xu, X. (2003). *Pm*AV, a novel gene involved in virus resistance of shrimp *Penaeus monodon*. *FEBS Lett.* **551:**53–57.

Mateu, M. G., Silva, D. A., Rocha, E., de Braum, D. L., Alonso, A., Enjuanes, L., Domingo, E., and Barahona, H. (1988). Extensive antigenic heterogeneity of foot-and-mouth disease virus serotype C. *Virology* **167:**113–124.

Mari, J., Bonami, J. R., and Lightner, D. V. (1998). Taura syndrome of penaeid shrimp: Cloning of viral genome fragments and development of specific gene probes. *Dis. Aquat. Org.* **33:**11–17.

Mari, J., Poulos, B. T., Lightner, D. V., and Bonami, J. R. (2002). Shrimp Taura syndrome virus: Economic characterization and similarity with members of the genus of cricket paralysis-like viruses. *J. Gen. Virol.* **83:**915–926.

Mayo, M. A. (2002). A summary of taxonomic changes recently approved by ICTV. *Arch. Virol.* **147:**1655–1656.

Mermoud, I., Costa, R., Ferre, O., Goarant, C., and Haffner, P. (1998). Syndrome 93′ in New Caledonian outdoor rearing ponds of *Penaeus stylirostris*: History and description of three major outbreaks. *Aquaculture* **164:**323–325.

Mohan, C. V., Shankar, K. M., Kulkarni, S., and Sudha, P. M. (1998). Histopathology of cultured shrimp showing gross signs of yellowhead syndrome and white spot syndrome during 1994 Indian epizootics. *Dis. Aquat. Org.* **34:**9–12.

Moore, N. F., Kearns, A., and Pullin, J. S. K. (1980). Characterization of cricket paralysis virus-induced polypeptides in *Drosophila* cells. *J. Virol.* **33:**1–9.

Moore, N. F., Reavy, B., and Pullin, J. S. K. (1981). Processing of cricket paralysis virus-induced polypeptides in *Drosophila* cells: Production of high molecular weight polypeptides by treatment with iodoacetamide. *Arch. Virol.* **68:**1–8.

Mouillesseaux, K. P., Klimpel, K. R., and Dhar, A. K. (2003). Improvement in the specificity and sensitivity of detection for the Taura syndrome virus and yellowhead virus of penaeid shrimp by increasing the amplicon size in SYBR Green real-time RT-PCR. *J. Virol. Methods* **111:**121–127.

Murphy, F. A., Fauquet, C. M., Bishop, D. H. L., Ghabrial, S. A., Jarvis, A. W., Martelli, G. P., Mayo, M. A., Summers, M. D. (eds.). (1995). Virus taxonomy, classification, and nomenclature of viruses. Sixth report of the international committee of taxonomy of viruses. *Arch. Virol.* **10** Suppl, Springer-Verlag, NewYork.

Nadala, E. C. B., Jr., Tapay, L. M., and Loh, P. C. (1997a). Yellowhead virus: A rhabdovirus-like pathogen of penaeid shrimp. *Dis. Aquat. Org.* **31:**141–146.

Nadala, E. C. B., Jr., Tapay, L. M., Cao, S., and Loh, P. C. (1997b). Detection of yellowhead virus and Chinese baculovirus in penaeid shrimp by the Western blot technique. *J. Virol. Methods* **69:**39–44.

Nadala, E. C. B., Jr., and Loh, P. C. (2000). Dot-blot nitrocellulose enzyme immunoassays for the detection of white spot virus and yellowhead virus of penaeid shrimp. *J. Virol. Methods* **84:**175–179.

Nash, G., Arkarjamon, A., and Withyachumnarnkul, B. (1995). Histological and rapid haemocytic diagnosis of yellowhead disease in *Penaeus monodon*. *In* "Diseases in Asian Aquaculture II" (M. Shariff, J. R. Arthur, and R. P. Subasinghe, eds.). Fish Health Section, Asian Fisheries Society, Manila, Philippines.

Natividad, K., Magbanua, F. O., Migo, V. P., Alfafara, C. G., Albaladejo, J. D., Nadala, E. C. B., Jr., Loh, P. C., and Tapay, L. M. (1999). Evidence of yellowhead virus in cultured black tiger shrimp (*Penaeus monodon* Fabricius) from selected shrimp farms in the Philippines. *Fourth Symposium on Diseases in Asian Aquaculture,* p. 60.

Nelsen-Salz, B., Zimmermann, A., Wickert, S., Arnold, G., Botta, A., Eggers, H. J., and Kruppenbacher, J. P. (1996). Analysis of sequence and pathogenic properties of two variants of encephalomyocarditis virus differing in a single amino acid in VP1. *Virus Res.* **41:**109–122.

Neumann, T., Kaiser, H. E., and Rath, F. W. (2000). A permanent cell line of the crayfish *Orconecte limosus* as a potential model in comparative oncology. *In vivo* **14:**691–698.

Nunan, L. M., Poulos, B. T., and Lightner, D. V. (1998). Reverse transcription polymerase chain reaction (RT-PCR) used for the detection of Taura syndrome virus (TSV) in experimentally infected shrimp. *Dis. Aquat. Org.* **34:**87–91.

Nunan, L., Poulos, B., Redman, R., Le Groumellec, M., and Lightner, D. V. (2003). Molecular detection methods developed for a systemic rickettsia-like bacterium (RLB) in *Penaeus monodon* (Decapoda: Crustacea). *Dis. Aquat. Org.* **53:**15–23.

OIE Fish Disease Commission (2002). *International Aquatic Animal Health Code*. 5th ed. Office International des Epizooties, Paris.

OIE Fish Disease Commission (2003). Yellowhead disease. Chap. 4.1.3 in Manual of diagnostic tests for aquatic animals. http://www.oie.int/eng/normes/fmanual/A_summry.htm.

Overstreet, R. M., Lightner, D. V., Hasson, K. W., McIlwain, S., and Lotz, J. (1997). Susceptibility to TSV of some penaeid shrimp native to the Gulf of Mexico and southeast Atlantic Ocean. *J. Invert. Path* **69:**165–176.

Owens, L. (1997). Special topic review: The history of the emergence of viruses in the Australian prawn industry. *World J. Microbiol. Biotechnol.* **13:**427–431.

Pantoja, C., and Lightner, D. V. (2001). Necrosis due to WSSV can mimic YHV lesions in lymphoid organ of penaeid shrimp. *Advocate* **4:**15.

Pantoja, C. R., and Lightner, D. V. (2003). Similarity between the histopathology of white spot syndrome virus and yellowhead syndrome virus and its relevance to diagnosis of YHV disease in the Americas. *Aquaculture* **218:**47–54.

Pasharawipas, T., Flegel, T. W., Sriurairatana, S., and Morrison, D. J. (1997). Latent yellowhead infections in *Penaeus monodon* and implications regarding disease resistance or tolerance. *In* "Shrimp Biotechnology in Thailand" (T. W. Flegel, P. Menasveta, and S. Paisarnrat, eds.). National Center for Biotechnology and Genetic Engineering, Bangkok, Thailand.

Phan, Y. T. N. (2001). Prevalence and coprevalence of white spot syndrome virus (WSSV) and yellowhead complex viruses (YHV-complex) in cultured giant tiger prawn (*Penaeus monodon*) in Vietnam. Master thesis. University of Queensland, Brisbane.

Poulos, B. T., Kibler, R., Bradley-Dunlop, D., Mohney, L. L., and Lightner, D. V. (1999). Production and use of antibodies for the detection of the Taura syndrome virus in penaeid shrimp. *Dis. Aquat. Org.* **37:**99–106.

Prior, S., and Browdy, C. L. (2000). Postmortem persistence of white spot and Taura syndrome viruses in water and tissue. *Proceedings for the Annual Conference of the World Aquaculture Society,* p. 397.

Prior, S., Segars, A., and Browdy, C. L. (2001). A preliminary assessment of live and frozen bait shrimp indicators and/or vectors of shrimp viruses. *The International and Triennial Conference and Exposition of the World Aquaculture Society,* p. 541.

Racusen, D. (1979). Glycoprotein detection in polyacrylamide gel with thymol and sulfuric acid. *Anal. Biochem.* **99:**474–476.

Robles-Sikisaka, R., Garcia, D. K., Klimpel, K. R., and Dhar, A. K. (2001). Nucleotide sequence of 3′-end of the genome of Taura syndrome virus of shrimp suggests that it is related to insect picornaviruses. *Arch. Virol.* **46:**941–952.

Robles-Sikisaka, R., Hasson, K. W., Garcia, D. K., Brovont, K. E., Cleveland, K., Klimpel, K. R., and Dhar, A. K. (2002). Genetic variation and immunohistochemical differences among geographic isolates of Taura syndrome virus of penaeid shrimp. *J. Gen. Virol.* **83:**3123–3130.

Roer, R. D., and Dillaman, R. M. (1993). Molt-related change in integumental structure and function. *In* "The Crustacean Integument: Morphology and Biochemistry" (M. N. Horst and J. A. Freeman, eds.). CRC Press, Boca Raton, LA.

Rojtinnakorn, J., Hirono, I., Itami, T., Takahashi, Y., and Aoki, T. (2002). Gene expression in hemocytes of kuruma prawn, *Penaeus japonicus*, in response to infection with WSSV by EST approach. *Fish Shellfish Immunol.* **13:**69–83.

Roux, M. M., Pain, A., Klimpel, K. R., and Dhar, A. K. (2002). Lipopolysaccharide and β-1,3-glucan-binding gene is upregulated in white spot virus (WSSV) infected in shrimp (*Penaeus stylirostris*). *J. Virol.* **76:**7140–7149.

Ruckert, R. R. (1996). Picornaviridae: The viruses and their replication. *In* "Field virology" (B. N. Fields, D. N. Knipe, and P. M. Howley, eds.). Lippincott-Raven, Philadelphia, PA.

Rukyani, A. (2000). Indonesia. *In* "Thematic Review on Management Strategies for Major Diseases in Shrimp Aquaculture" (J. R. Arthur, D. Fegan, and R. Subasinghe, eds.). FAO, Rome, Italy.

Sasaki, J., and Nakashima, N. (1999). Translation initiation at the CUU codon is mediated by the internal ribosomal entry site of an insect picorna-like virus *in vitro*. *J. Virol.* **73:**1219–1226.

Sasaki, J., and Nakashima, N. (2000). Methionine-independent initiation of translation in the capsid protein of an insect RNA virus. *Proc. Natl. Acad. Sci.* **97:**1512–1515.

Sasaki, J., Nakashima, N., Saito, H., and Noda, H. (1998). An insect picorna-like virus, *Plautia stali* intestine virus, *has* genes of capsid proteins in the 3′-part of the genome. *Virology* **244:**50–58.

Sawicki, S. G., and Sawicki, D. L. (1999). A new model for coronavirus transcription. *Adv. Exp. Med. Biol.* **440:**215–219.

Siriwardena, P. P. G. S. N. (2000). Sri Lanka. *In* "Thematic Review on Management Strategies for Major Diseases in Shrimp Aquaculture" (J. R. Arthur, D. Fegan, and R. Subasinghe, eds.). FAO, Rome, Italy.

Sithigorngul, P., Chauychuwong, P., Sithigorngul, W., Longyant, S., Chaivisuthangkura, P., and Menasveta, P. (2000). Development of a monoclonal antibody specific to yellowhead virus (YHV) from *Penaeus monodon*. *Dis. Aquat. Org.* **42:**27–34.

Sithigorngul, P., Rukpratanporn, S., Longyant, S., Chaivisuthangkura, P., Sithigorngul, W., and Menasveta, P. (2002). Monoclonal antibodies specific to yellowhead virus (YHV) of *Penaeus monodon*. *Dis. Aquat. Org.* **49:**71–76.

Sittidilokratna, N. (2003). Analysis of the YHV Genome and Expression of Recombinant Glycoprotein. gp116. Ph.D. diss. Mahidol University, Bangkok.

Sittidilokratna, N., Hodgson, R. A. J., Cowley, J. A., Jitrapakdee, S., Boonsaeng, V., Panyim, S., and Walker, P. J. (2002). Complete ORF1b-gene sequence indicates yellowhead virus is an invertebrate nidovirus. *Dis. Aquat. Org.* **50:**87–93.

Siveter, D. J., Williams, M., and Waloszek, D. (2001). A phosphatocopid crustacean with appendages from the Lower Cambrian. *Science* **293:**479–481.

Smith, P. T. (2000). Diseases of the eye of farmed shrimp *Penaeus monodon*. *Dis. Aquat. Org.* **43:**159–173.

Snijder, E. J., and Meulenberg, J. J. M. (1998). The molecular biology of arteriviruses. *J. Gen. Virol.* **79:**961–979.

Soowannayan, C., Sithigorngul, P., and Flegel, T. W. (2002). Use of a specific monoclonal antibody to determine tissue tropism of yellowhead virus (YHV) of *Penaeus monodon* by *in situ* immunohistochemistry. *Fish Science* **68**(Suppl. 1):805–809.

Soowannayan, C., Flegel, T. W., Sithigorngul, P., Slater, J., Hyatt, A., Cramerri, S., Wise, T., Crane, M. S. J., Cowley, J. A., McCulloch, R. J., and Walker, P. J. (2003). Detection and differentiation of yellowhead complex viruses using monoclonal antibodies. *Dis. Aquat. Org*. **57:**193–200.

Spann, K. M., Vickers, J. E., and Lester, R. J. G. (1995). Lymphoid organ virus of *Penaeus monodon* from Australia. *Dis. Aquat. Org.* **23:**127–134.

Spann, K. M., Cowley, J. A., Walker, P. J., and Lester, R. J. G. (1997). A yellowhead-like virus from *Penaeus monodon* in Australia. *Dis. Aquat. Org.* **31:**169–179.

Spann, K. M., Donaldson, R. A., Cowley, J. A., and Walker, P. J. (2000). Differences in the susceptibility of some penaeid prawn species to gill-associated virus (GAV) infection. *Dis. Aquat. Org.* **4:**221–225.

Spann, K. M., McCulloch, R. J., Cowley, J. A., East, I. J., and Walker, P. J. (2003). Detection of gill-associated virus (GAV) by *in situ* hybridization during acute and chronic infections of *Penaeus monodon* and *P. esculentus*. *Dis. Aquat. Org.* **56:**1–10.

Stern, S. (1995). Swimming through troubled waters in shrimp farming: Ecuador country review. *In* "Swimming through Troubled Water" (C. L. Browdy and J. S. Hopkins, eds.). Proceedings of the Special Session on Shrimp Farming Aquaculture, World Aquaculture Society, Baton Rouge, LA.

Tang, K. F. J., and Lightner, D. V. (1999). A yellowhead virus gene probe: Nucleotide sequence and application for *in situ* hybridization. *Dis. Aquat. Org.* **35:**165–173.

Tang, K. F. J., Spann, K. M., Owens, L., and Lightner, D. V. (2002). *In situ* detection of Australian gill-associated virus with a yellowhead virus gene probe. *Aquaculture* **205:**1–5.

Tang, K. F. J., Wang, J., and Lightner, D. V. (2003). Quantitation of Taura syndrome virus by real-time RT-PCR with a TaqMan assay. *J. Virol. Methods* **115:**109–114.

Toullec, J. (1999). Crustacean primary cell culture: A technical approach. *Methods Cell Sci.* **21:**193–198.

Tu, C., Huang, H., Chuang, S., Hsu, J., Kuo, S., Li, N., Hsu, T., Li, M., and Lin, S. (1999). Taura syndrome in pacific white shrimp *Penaeus vannamei* cultured in Taiwan. *Dis. Aquat. Org.* **38:**159–161.

van de Braak, C. B. T., Botterblom, M. H. A., Taverne, N., Van Muiswinkel, W. B., Rombut, J. H. W. M., and van der Knapp, W. P. W. (2002). The roles of hemocytes and the lymphoid organ in the clearance of injected *Vibrio* bacteria in *Penaeus monodon* shrimp. *Fish Shell. Immunol.* **13:**293–309.

van der Wilk, F., Dullemans, A. M., Verbeek, M., and van den Heuvel, J. F. (1997). Nucleotide sequence and genomic organization of *Acyrthosiphon pisum* virus. *Virology* **238:**353–362.

van Marle, G., Dobbe, J. C., Gultyaev, A. P., Luytjes, W., Spaan, W. J. M., and Snijder, E. J. (1999). Arterivirus discontinuous mRNA transcription is guided by base pairing between sense and antisense transcription-regulating sequences. *Proc. Natl. Acad. Sci. USA* **96:**12056–12061.

van Regenmortel, M. H. V., Fauquet, C. M., Bishop, D. H. L., Carstens, E. B., Estes, M. K., Lemon, S. M., Maniloff, J., Mayo, M. A., McGeoch, D. J., Pringle, C. R., and Wickner, R. B. (2000). "Virus Taxonomy: The Classification and Nomenclature of Viruses." *The seventh Report of the International Committee on Taxonomy of Viruses*. Academic Press, San Diego, CA.

van Vliet, A. L., Smits, S. L., Rottier, P. J., and de Groot, R. J. (2002). Discontinuous and nondiscontinuous subgenomic RNA transcription in a nidovirus. *EMBO J.* **21:**6571–6580.

Walker, P. J., Cowley, J. A., Spann, K. M., Hodgson, R. A. J., Hall, M. R., and Withyachumnarnkul, B. (2001). Yellowhead complex viruses: Transmission cycles and topographical distribution in the Asia-Pacific region. *In* "The New Wave" (C. L. Browdy and D. E. Jory, eds.). *Proceedings of the Special Session on Sustainable Shrimp Culture*. The World Aquaculture Society, Baton Rouge, LA.

Walker, P. J., Flegel, T. W., Boonsaeng, V., Lightner, D. V., Tang, K. F. J., Loh, P. C., Chang, P. S., Bonami, J. R., Cowley, J. A., Snijder, E. J., and Enjuanes, L. (2003). Roniviridae. Taxonomic structure of the family. *In* "Virus Taxonomy, Eighth Report of the International Committee on Taxonomy of Viruses" (M. H. V. van Regenmortel, C. M. Fauquet, D. H. L. Bishop, E. B. Estes, S. M. Lemon, J. Maniloff, M. A. Mayo, D. J. McGeoch, C. R. Pringle, and R. B. Wickner, eds.). Academic Press, San Diego, CA.

Wang, C. S., Tang, K. J., Kuo, G. H., and Chen, S. N. (1996). Yellowhead disease-like virus infection in the Kuruma shrimp *Penaeus japonicus* cultured in Taiwan. *Fish. Pathol.* **31:**177–182.

Wang, Y. C., and Chang, P. S. (2000). Yellowhead virus infection in the giant tiger prawn *Penaeus monodon* cultured in Taiwan. Fish. *Pathol.* **35:**1–10.

Wigglesworth, J. (1994). Taura Syndrome hits Ecuador farms. *Fish Farmer* **17:**30–31.

Wilson, J. E., Powell, M. J., Hoover, S. E., and Sarnow, P. (2000). Naturally occurring dicistronic cricket paralysis virus RNA is regulated by two internal ribosomal entry sites. *Mol. Cell. Biol.* **20:**4990–4999.

Wongteerasupaya, C., Boonsaeng, V., Panyim, S., Tassanakajon, A., Withyachumnarnkul, B., and Flegel, T. W. (1997). Detection of yellowhead virus (YHV) of *Penaeus monodon* by RT-PCR amplification. *Dis. Aquat. Org.* **31:**181–186.

Wongteerasupaya, C., Sriurairatana, S., Vickers, J. E., Anutara, A., Boonsaeng, V., Panyim, S., Tassanakajon, A., Withyachumnarnkul, B., and Flegel, T. W. (1995). Yellowhead virus of *Penaeus monodon* is an RNA virus. *Dis. Aquat. Org.* **22:**45–50.

Yang, Y. G., Shariff, M., Lee, L. K., and Hassan, M. D. (2000). Malaysia. *In* "Thematic Review on Management Strategies for Major Diseases in Shrimp Aquaculture" (J. R. Arthur, D. Fegan, and R. Subasinghe, eds.). FAO, Rome, Italy.

Yu, C., and Song, Y. (2000). Outbreaks of Taura syndrome in Pacific white shrimp *Penaeus vannamei* cultured in Taiwan. *Fish Pathol.* **35:**21–24.

Zarain-Herzberg, M., and Ascencio-Valle, F. (2001). Taura syndrome in Mexico: Follow-up study in shrimp farms of Sinaloa. *Aquaculture* **193:**1–9.

Ziebuhr, J., Bayer, S., Cowley, J. A., and Gorbalenya, A. E. (2003). The 3C-like proteinase of an invertebrate nidovirus links coronavirus and potyvirus homologs. *J. Virol.* **77:**1415–1426.